FosL1 determines the differential signaling by TLR7 and TLR8 during RNA virus infection

Marine de Marcken[1], Khushwant Dhaliwal[1], Ann Caroline Danielsen[1], Anne Sophie Gautron[1] and Margarita Dominguez-Villar[1,#,*]

One-sentence summary: Identification of FOSL1 as a mediator of TLR7 and TLR8 signaling differences in human monocytes

1 Department of Neurology, Yale School of Medicine, New Haven, Connecticut, 06520

* Current address: Department of Medicine, Imperial College London, W2 1PG London, UK

Corresponding author. Email: margarita.dominguez-villar@yale.edu, m.dominguez-villar@imperial.ac.uk

Abstract

Human blood $CD14^+$ monocytes are bone-marrow derived leukocytes that sense and respond to pathogens. While initial innate immune activation by RNA viruses preferentially occurs via RLR, other nucleic acid recognition receptors, such as TLRs, play a role in finely programming the final outcome of virus-antigen presenting cell interaction. Here, we dissected the phenotype of monocytes after infection with various RNA viruses and the involvement of TLR7 and TLR8. We found that TLR7 and TLR8 activated differential signaling cascades that contributed to the distinct phenotypes observed. We found that FOSL1 inhibited type 1 cytokines after TLR7 signaling and we uncovered the role of TLR7-dependent Ca^{2+} flux in modulating type I IFN responses. Our work demonstrated that although both TLR7 and TLR8 recognize single-stranded RNA, they triggered different signaling pathways in human monocytes that contribute to distinct phenotypes during RNA virus infection. In addition, we defined individual targets within these pathways that promoted specific T helper and antiviral responses.

Introduction

Human monocytes are bone marrow-derived leukocytes from the innate immune system with important functions in pathogen sensing during bacterial, viral and fungal infections. Monocytes are broadly classified based on the expression of CD14 and CD16 into classical ($CD14^+$), intermediate ($CD14^+CD16^+$) and non-classical ($CD14^{low}CD16^+$) monocytes(*1, 2*), although single-cell transcriptomic data suggest that monocytes are likely much more heterogeneous(*3*). $CD14^+$ classical monocytes are the most abundant population, representing 80-90% of circulating monocytes(*4*) and have been shown to produce pro-inflammatory cytokines, phagocytose and secrete reactive oxygen species (ROS) upon pathogen sensing(*2*).

During the course of a viral infection, circulating monocytes rapidly leave the bloodstream and migrate to tissues where, following pathogen sensing and/or other stimuli, they differentiate into macrophages or dendritic cells(*4*). This recruitment is essential for effective control, and ultimately, clearance of the infection. However, in addition to this function, monocytes can also exert direct antimicrobial responses and promote the adaptive immune response. Monocytes are equipped with pattern recognition and phagocytic receptors necessary for pathogen sensing and destruction and they also produce pro-inflammatory cytokines, which may help initiate the adaptive immune response(*4*).

Although peripheral blood monocytes are a major population targeted by viruses during host infection(*5-9*), little is known about the early events that are triggered when RNA viruses interact with human monocytes, and how these interactions modulate the phenotype and effector functions of the latter. Among the pattern recognition receptors expressed by monocytes, nucleic acid sensing receptors have been identified as major components triggering cell activation during RNA virus infection(*10*). RIG-I-like receptors (RLRs) such as MDA5, RIG-I and LPG2, are

cytoplasmic sensors of RNA(*11*), whereas toll-like receptors (TLR) 7 and 8 are intracellular sensors located in endosomes that recognize single-stranded RNA. Both types of receptors induce the expression of pro-inflammatory cytokines and type I IFN response upon RNA virus sensing(*11, 12*). Monocytes from healthy individuals express RLRs(*13*) and both TLR7(*14*) and TLR8(*15*), and their expression can vary in patients with infectious diseases as compared to healthy individuals(*16, 17*).

In this study we examined the signaling pathways downstream TLR7 and TLR8 that occur after monocyte interaction with RNA viruses ex vivo and their capacity to drive specific cytokine production leading to the regulation of the adaptive immune response. We demonstrated that RNA virus infection induced a variety of phenotypes and distinct antiviral responses in human monocytes as a result of the simultaneous activation of various pattern recognition receptors. We focused on the role of TLR7 and TLR8 signaling and we demonstrated that even though both receptors recognize the same generic ligand, there were important differences between their activation. TLR7 preferentially mediated the expression of Th17-polarizing cytokines after virus infection, while Th1-type cytokine production and type I IFN response were dependent on TLR8 signaling. The differences in pro-inflammatory cytokine expression induced by TLR7 or TLR8 signaling were due to the TLR7-dependent upregulation of Fos family member FOSL1, which inhibited type 1 cytokine expression. Furthermore, we uncovered a role for TLR7-dependent Ca^{2+} flux in inhibiting type I IFN responses. In conclusion, our work demonstrates that although TLR7 and TLR8 both recognize single-stranded RNA, they trigger different signaling pathways in human monocytes that contribute to distinct phenotypes during RNA virus infection. In addition, we define specific targets within these pathways susceptible to modulation for induction of specific T helper and antiviral responses.

Results

RNA virus infection of monocytes induces virus-specific phenotypes.

Circulating monocytes display distinct phenotypes in patients with different RNA virus infections, and while monocytes are a major population infected by viruses in peripheral blood(*18*), the early events that occur after interactions of viruses with monocytes are poorly understood. To examine this, ex vivo isolated $CD14^+$ classical monocytes from healthy individuals were infected with several RNA viruses for 16 hours at an MOI of 5. The chosen viruses, i.e. Coxsackie virus (CV)(*19, 20*), Encephalomyocarditis virus (EMCV)(*21, 22*), Influenza A Virus (IAV)(*23, 24*), Measles virus (MV)(*25*), Sendai virus (SV)(*26, 27*) and Vesicular Stomatitis virus (VSV)(*28, 29*) have all been shown to either be passively internalized by or actively infect monocytes in vivo and/or in vitro. As a readout, we decided to examine two main monocyte functions: T cell polarizing capacity by the expression of specific pro-inflammatory cytokines, and antiviral response, measured by the expression of type I interferon (IFN) and IFN-stimulated genes (ISGs, Fig 1). For Th1-type cytokines, we assessed the expression of *IL12B*, *IL18*, *IL27*, and *TNF*, and for Th17-polarizing cytokines we examined *IL1B*, *IL6*, *IL23A*, and *TGFB1*. As expected, human monocytes were rapidly activated in the presence of RNA viruses and produced pro-inflammatory and antiviral cytokines in a virus-specific fashion (Fig 1). Some viruses preferentially induced the secretion of Th1-polarizing cytokines, such as EMCV, while others, such as MV and VSV preferentially upregulated the expression of Th17-polarizing cytokines. Other viruses, such as IAV, induced the expression of both types of cytokines (Fig 1A). These distinct gene expression patterns were confirmed at protein level by measuring cytokine release in the culture supernatant (Fig 1B).

With regards to the type I IFN response, there was a striking variability in the levels of *IFNA* and *IFNB* gene expression upon virus infection. Thus, while some viruses such as EMCV, VSV or IAV significantly increased the expression of both cytokines, some other viruses, such as MV, CV or SV did not (Fig 1C). *IFNA* and *IFNB* expression correlated with the increased expression levels

of ISGs, and thus, EMCV, VSV and IAV infections displayed a significant increased expression of ISGs, while CV barely induced the expression of any ISGs and MV and SV displayed low but detectable levels of ISGs (Fig 1C). The results were confirmed at protein level by measuring IFNα and IFNβ in the culture supernatant (Fig 1D).

These data suggest that early interactions of RNA viruses with human $CD14^+$ monocytes trigger the expression of pro-inflammatory cytokines and antiviral response in a virus-specific fashion.

Single-stranded RNA-sensing TLRs contribute to the differential phenotype observed after RNA virus infection.

During infection of APCs, RNA viruses are first sensed by host cells through several pattern recognition receptors(*30*), with a major contribution of those sensors that recognize viral nucleic acids(*31*), and in particular, RLRs. Subsequently, nucleic acid-specific Toll-like receptors are also involved in fine tuning of the immune response after RLR innate activation(*11*). We decided to examine the contribution of single-stranded RNA-sensing TLR (TLR7 and TLR8) to the cytokine patterns observed after infection of monocytes. TLR7 and TLR8 are both expressed by $CD14^+$ monocytes ex vivo and upregulated soon after virus encounter(*14, 32, 33*) (fig S1). In order to test their involvement in monocyte activation we blocked each of them individually with two inhibitory sequences that have been shown to be specific for TLR7 (IRS661)(*34*) and TLR8 (IRS957)(*35, 36*) in human monocytes. We incubated ex vivo isolated $CD14^+$ monocytes with IRS661 or IRS957 for 30 min prior to infection with RNA viruses for 16 hours, and we examined pro-inflammatory cytokine gene expression by real-time PCR and protein secretion by ELISA (Fig 2). Both TLR7 and TLR8 blockade had virus- and cytokine-specific effects. TLR8 blockade did not inhibit the expression of *IL1B* nor *IL23A*, and in some instances there was a trend towards increased expression, suggesting either a negative, or no role for TLR8 in *IL1B* nor *IL23A* expression during

virus infection. In contrast, in those virus infections that induced Th17-polarizing cytokines (IAV, MV, VSV), TLR7 blockade significantly decreased *IL1B* and *IL23A* expression while having no effect on EMCV, SV and CV infections. The regulation of *IL6* expression by TLR7 and TLR8 was virus-specific, and while TLR7 blockade had no effect on *IL6* expression upon CV, EMCV, SV or VSV infections, it decreased *IL6* expression in MV and IAV infections. Similarly, TLR8 blockade had no effect on *IL6* expression triggered by all viruses except for EMCV, where it led to decreased gene expression (Fig 2A). Blockade of both TLR7 and TLR8 by the simultaneous use of IRS661 and IRS957 did not completely abrogate cytokine expression, supporting the involvement of other pattern recognition receptors, and RLR in particular, in innate immune cell activation after RNA infection (fig S2).

TLR7 and TLR8 had different effects on Th1-polarizing cytokine expression. While TLR7 blockade had no effect on the expression of *IL12B*, *IL27* or *TNF* triggered by any virus, TLR8 blockade significantly decreased the expression of *IL12B* and *IL27* in CV, EMCV, MV and SV infections. *TNF* was also inhibited in EMCV and IAV infections in the presence of IRS957, suggesting a role of TLR8 on the modulation of Th1-type cytokines during virus infection (Fig 2A). TLR7 and TLR8 silencing in monocytes and subsequent virus infection confirmed the results obtained with IRS661 and IRS957 (fig S3). Cytokine secretion data assessed by ELISA supported the gene expression results and suggested that TLR7 was involved in the expression of Th17-polarizing cytokines (IL-1β, IL-6 and IL23) upon viral infection, while TLR8 controlled the expression of Th1-type cytokines (IL-27, TNFα) and IL-6 (Fig 2B).

TLR7 signaling does not contribute to the type I IFN response triggered by viruses during CD14$^+$ monocyte infection.

We went on to examine the involvement of TLR7 and TLR8 signaling on the generation of a type I IFN response during virus infection. Monocytes were pre-incubated with IRS661 and IRS957 and infected with RNA viruses as above, and we determined the expression of *IFNA1*, *IFNA2* and *IFNB1* by real-time PCR (Fig 3A). Whereas TLR8 blockade significantly inhibited the expression of the genes in most virus infections, TLR7 blockade did not modify *IFNA1*, *IFNA2* or *IFNB1* gene expression, and in some cases, as in EMCV infection, significantly increased them. These results were confirmed at protein level by measuring IFNα and IFNβ cytokines in the culture supernatant (Fig 3B). Furthermore, the expression of the ISGs *EIF2AK2*, *IFITM1*, *ISG15*, *MOV10* and *TRIM5* was decreased by TLR8 blockade, while no effect was observed upon TLR7 blockade, with the exception of a slight inhibition of *IFITM1* and *ISG15* expression upon MV infection, and *EIF2AK2* and *ISG15* upon SV infection (Fig 3C). TLR7- and TLR8-silencing further confirmed the absence of involvement of TLR7 in the type 1 IFN response upon RNA virus infection, and the role of TLR8 in triggering it (fig S4).

TLR7 triggering induces a Th17-polarizing phenotype while TLR8 stimulation induces a Th1-polarizing phenotype on human CD14$^+$ monocytes.

The different effects of TLR7 and TLR8 inhibition on pro-inflammatory cytokine expression and type I IFN responses led us hypothesize that TLR7 and TLR8 stimulation induce different functional phenotypes on CD14$^+$ monocytes. To test this hypothesis, we chose imiquimod (IMQ) as a human TLR7-specific ligand and ssRNA40-LyoVec (ssRNA40) as a human TLR8-specific ligand and we stimulated ex vivo isolated CD14$^+$ monocytes with them to examine the expression of pro-inflammatory cytokines (Fig 4). In agreement with the inhibition experiments, IMQ treatment induced the expression of *IL1B*, *IL6*, *IL23A* and *TGFB1* but failed to increase the expression of *IL12B*, *IL18*, *IL27* or *TNF*. On the contrary, Th1-type cytokine gene expression was significantly increased after ssRNA40 stimulation. TLR8 triggering also increased the expression of *IL6* and *IL1B*, albeit at much lower levels as compared to TLR7 stimulation (Fig 4A). These differences

were not due to a kinetics issue, as IMQ did not induce *IL12B*, *IL27* or *TNF* expression at any time point examined during the 24 hours of stimulation (fig S5A). Moreover, the differences in protein expression were not due to differences in cell numbers, as confirmed by flow cytometry (fig S5, B and C). To determine whether the distinct cytokine expression patterns by IMQ and ssRNA40 were due to the specific concentrations of IMQ or ssRNA40 used, we stimulated monocytes with various concentrations of each TLR ligand covering the concentration ranges recommended by the manufacturer. Supernatant from the cultures were used to determine IL-1β, IL-6, IL-12 and TNFα secretion by ELISA (Fig 4B). While TLR8 stimulation induced the secretion of all cytokines examined, IMQ-stimulated monocytes did not secrete IL-12 at any concentration tested and it only induced a detectable amount of TNFα with the highest concentration used (328±177 pg/ml with 10 μg/ml IMQ as compared to 4960±935 pg/ml with 5 μg/ml ssRNA40). The different cytokine production patterns were TLR7- and TLR8-specific, as TLR7 blockade with IRS661 inhibited IMQ-dependent secretion of IL-1β and IL-6, but not TNFα, and had no effect on cytokines released by ssRNA40-stimulated monocytes. In contrast, TLR8 blockade with IRS957 significantly decreased the secretion of IL-6 and TNFα but not IL-1β release upon ssRNA40 stimulation, while not affecting the production of IL-1β nor TNFα, and increasing IL-6 secretion after IMQ stimulation (Fig 4C).

To further confirm the specificity of our results, we stimulated monocytes with other human TLR7- and TLR8-specific ligands, including Gardiquimod (GDQ) and Loxoribine (Loxo) as TLR7 ligands, and ssRNA-DR and PolyU as TLR8-specific ligands. Gene expression analysis of Th1- and Th17-type cytokines confirmed that TLR7 ligands preferentially induce *IL1B*, *IL6* and *IL23A*, while TLR8 ligands increase the expression of *IL12B*, *IL27*, *TNF* (Fig 4D), and this was confirmed at protein level in the culture supernatant (fig S5D). Furthermore, we examined the expression of surface receptors and chemokines that have been associated to type 1 and type 17 responses. Thus,

TLR8 stimulation did not upregulate *ICOSLG*, which is important for human Th17 differentiation(*37*), and upregulated the Th1-related receptor CD40(*38*). In contrast, TLR7 signaling slightly increased the expression of ICOSL, and it failed to upregulate CD40 at RNA and protein levels (Fig 4, D, E and F). Moreover, IMQ-treated monocytes significantly upregulated the expression of the chemokine *CCL20*, the ligand for CCR6, which is preferentially expressed by Th17 cells(*39*). In contrast, ssRNA40-stimulated monocytes upregulated *CXCL10* expression, the ligand for the chemokine receptor CXCR3, which is preferentially expressed by Th1 cells(*40*).

To functionally confirm the capacity of TLR7- and TLR8-stimulated monocytes to induce Th17 and Th1 cells, respectively, we stimulated monocytes with IMQ, ssRNA40 or vehicle and subsequently co-cultured them with $CD4^+$ T cells isolated from the same donors in the presence of only anti-CD3, to allow monocytes to provide the costimulatory signals under a similar polyclonal TCR stimulation (Fig 5). Subsequently, $CD4^+$ T cells were sorted by flow cytometry to examine the expression of Th1- (*IFNG* and *TBX21*), Th2- (*IL4* and *GATA3*), Th17- (*IL17A* and *RORC*) and Treg-related (*FOXP3* and *IL10*) cytokines and transcription factors. $CD4^+$ T cells that were co-cultured with ssRNA40-treated monocytes displayed a significantly increased expression of *IFNG* and *TBX21* and decreased expression of *GATA3* and *RORC* as compared to $CD4^+$ T cells stimulated with vehicle-treated monocytes. However, $CD4^+$ T cells co-cultured with IMQ-treated monocytes failed to induce *IFNG* or *TBX21*, but significantly increased the expression of *IL17A* and *RORC*. No differences were observed in the expression of *FOXP3* or *IL10* by $CD4^+$ T cells in any co-culture (Fig 5A). Cytokine release in the co-cultures measured by ELISA confirmed that IFNγ was only detected in the co-cultures with ssRNA40-treated monocytes, and IL-17 was preferentially secreted in co-cultures with IMQ-treated monocytes (Fig 5B). The lack of Th1 cell induction by IMQ-treated monocytes was also confirmed at early and late time points during the co-culture period (fig S5E).

TLR7 preferentially signals though MAPK and displays defective NFkB activation

A common feature of most TLR signaling pathways is the activation of 3 major transcription factors. i.e. AP-1 and NFκB, responsible for pro-inflammatory cytokine release, and IRF3, involved in the antiviral type I IFN response(*41*). We examined whether the differences in pro-inflammatory cytokine secretion patterns elicited by TLR7 and TLR8 stimulation were due to differences in their capacity to activate AP-1 and NFκB. For this, we stimulated human $CD14^+$ monocytes with IMQ, ssRNA40 and we measured the expression of phosphorylated MKK3/6, MKK4/7 and MEK1/2 (Fig 6). MKKs and MEKs belong to the MAPK family and are involved in the activation of p38, JNK and ERK, whose phosphorylation leads to AP-1 activation and secretion of pro-inflammatory cytokines(*42*). MKK3/6 and MKK4/7 were rapidly activated upon IMQ or ssRNA40 stimulation at comparable levels. However, there was a small but significant increase in the phosphorylation of MEK1/2 upon IMQ stimulation at 5 and 15 min that was not observed after ssRNA40 stimulation (Fig 6, A and B). Subsequently we assessed the expression of phosphorylated p38 and ERK1/2 after IMQ or ssRNA40 activation. TLR7 induced an increase in phospho-p38 at all time points examined except for 60 min, whereas TLR8 stimulation only induced a modest increase at 5 and 30 min. The differences in p38 phosphorylation between IMQ and ssRNA40-stimulated monocytes were statistically significant at all time points examined except for 60 min. Furthermore, while TLR8 failed to increase phospho-ERK1/2 expression as compared to vehicle-treated cells, TLR7-stimulated monocytes displayed a sharp increase in phospho-ERK1/2 expression 5 min after stimulation (Fig 6, C and D). These data suggest that TLR7 signaling induces MAPK activation more effectively than TLR8 signaling, in agreement with the increased IL-1β and IL-23 production observed, which are partially regulated by AP-1(*43, 44*).

We went on to examine NFκB activation upon TLR7 and TLR8 stimulation. NFκB is a homo- or heterodimer of NFκB or Rel proteins. In resting cells, NFκB remains in the cytoplasm in an inactive

state, complexed with the inhibitory protein IκBα. TLR triggering leads to activation of NFκB by both phosphorylation of its subunits and ubiquitination-mediated proteasomal degradation of IκBα, which leads to NFκB translocation to the nucleus(*45, 46*). We assessed NFκB activation by p65 subunit phosphorylation and IκBα degradation (Fig 6, E and F). p65 phosphorylation showed a significantly different kinetics on TLR7- as compared to TLR8-stimulated monocytes. While ssRNA40 induced a robust activation of p65 maintained during 60 min of activation, IMQ-stimulated monocytes displayed a modest p65 activation at 15 and 30 min that rapidly vanished. Significant differences in phospho-p65 were observed at 45 and 60 min after activation when comparing IMQ- vs ssRNA40-treated monocytes (Fig 6F). IκBα expression correlated with the differences in p65 phosphorylation. Thus, while ssRNA40 induced a significant decrease in the expression of IκBα by 30 min of activation, this was almost absent in IMQ-treated monocytes and there was only a significant decrease in its expression at 60 min, supporting the observation that TLR7 stimulation fails to induce robust NFκB activation, and consequently, the expression of the type 1 cytokines that are dependent on NFκB function, such as TNFα(*47, 48*), IL-12(*49*) and IL-27(*50, 51*).

FOSL1 inhibits type 1 cytokines after TLR7 stimulation

AP-1 transcription factors are a family of heterodimers predominantly composed of one member of each of two major families of proteins: FOS (c-FOS, FOSL1, FOSL2, FOSB) and JUN (c-JUN, JUNB, JUND). In addition, members of the ATF and MAF families can replace in some instances one of the FOS or JUN proteins in the dimer(*52*). AP-1 regulation occurs both transcriptionally and post-translationally after exposure to several different stimuli(*53*). Among them, TLR ligation rapidly induces their increased expression(*54*). We examined the expression of AP-1 subunits elicited by ssRNA40 and IMQ as compared to vehicle-treated monocytes. The expression of all JUN family genes was similarly increased by either IMQ or ssRNA40 when compared to control

(fig S6A); however, there were significant differences in the expression of *ATF1*, *ATF2*, *FOSL1* and *FOSL2*. Monocytes stimulated with TLR7 upregulated all 4 transcription factors as compared to vehicle-treated monocytes, whereas TLR8-stimulated cells decreased *ATF1* and *ATF2*, and slightly increased *FOSL2* expression when compared to vehicle-stimulated monocytes. ssRNA40 had no effect on *FOSL1* expression (Fig 7A).

Unlike the rest of the FOS family, FOSL1 and FOSL2 proteins lack transactivation domains and have been suggested to display weak transactivation potentials. Under certain circumstances they even act as negative regulators of AP-1 activity by competing for binding to AP-1 sites or by dimerizing with JUN and forming "inactive" heterodimers(*53, 55, 56*). Based on these observations and the fact that type 1 cytokines, which require AP-1 activation(*50, 57-63*), were not produced after TLR7 signaling, we hypothesized that upregulation of *FOSL1* and/or *FOSL2* negatively regulated type 1 cytokines. To test this, we silenced *ATF1*, *ATF2*, *FOSL1* and *FOSL2* on $CD14^+$ monocytes (fig S6B) and we subsequently stimulated them with either vehicle or IMQ. Gene expression analysis demonstrated that *ATF1*, *ATF2* and *FOSL2* silencing significantly decreased the expression of *IL1B* and *IL6* following TLR7 stimulation, suggesting redundant roles for these transcription factors in the expression of type 17 cytokines (fig S6C). *IL23A* expression was decreased on *ATF2*-silenced monocytes as compared to controls after IMQ treatment, suggesting a positive role for ATF2 in *IL23A* transcription. Genetic deletion of *FOSL1* had no effect on any of the type 17 cytokines measured. However, when we examined the expression of type 1 cytokines (Fig 7B), *FOSL1* silencing significantly increased the expression of *IL12B*, *IL27* and *TNF* after IMQ treatment, as compared to non-target (NT)-transfected cells. *ATF1*, *ATF2* and *FOSL2* silencing had no effect on type 1 cytokine expression after IMQ stimulation. We confirmed the inhibitory effects of FOSL1 on type 1 cytokine secretion by measuring IL-27 and TNFα secretion in the culture supernatant from *FOSL1*-silenced monocytes (Fig 7C).

As TLR7 and TLR8 displayed non-overlapping roles in the secretion of specific cytokines upon RNA virus infections (Fig 1), we decided to examine the expression of *FOSL1* in monocytes stimulated with RNA viruses. We observed a significant upregulation of *FOSL1* after IAV, MV and VSV infections as compared to vehicle-treated monocytes (Fig 7D), which displayed a more Th17-polarizing capacity that was partly TLR7-dependent (Fig 2). To examine whether virus-induced *FOSL1* regulates the expression of type 1 cytokines, we stimulated *FOSL1*- or *NT*-silenced monocytes with IAV, MV and VSV and examined the expression of *IL-27* and *TNF*. *FOSL1*-silenced cells increased *TNF* expression upon IAV and VSV infections, although only IAV reached statistical significance. Moreover, *IL27* was increased in *FOSL1*-silenced monocytes after IAV and MV infection. These data suggest that RNA viruses that signal through TLR7 upregulate *FOSL1* to restrain type 1 pro-inflammatory cytokine production (Fig 7E).

TLR7 signaling does not induce a type I IFN response in human CD14$^+$ monocytes.

An important function of APCs is their antiviral capacity upon RNA virus infection by the secretion of type I IFN and ISGs(*64*). Monocytes infected with several RNA viruses secreted type I IFN in a TLR7-independent manner (Fig 3). To examine whether direct stimulation through TLR7 induced a type I IFN response, CD14$^+$ monocytes were stimulated ex vivo with IMQ or ssRNA40 for 36 hours and the expression of *IFNA1*, *IFNA2* and *IFNB1* was examined at various time points (Fig 8A). Although IMQ did not upregulate any of the three cytokines at any time point, ssRNA40 induced all three with different expression kinetics. These data were confirmed at protein level by measuring IFNα and IFNβ in the culture supernatant (Fig 8B). The lack of IFN response after TLR7 stimulation was not due to the specific concentration of IMQ used, as none of the various concentrations tested within the recommended range induced significant expression of any of the IFN cytokines (Fig 8C), while increasing amounts of ssRNA40 increased the expression of *IFNA1*, *IFNA2* and *IFNB1*. We confirmed these results at protein level by measuring IFNα and IFNβ in

the culture supernatant (Fig 8D). Accordingly, the expression of ISGs was virtually absent in IMQ-stimulated monocytes, while TLR8 activation induced a significant increase in the expression of the 6 ISG tested (Fig 8E). To confirm that the defect in IFN expression upon IMQ stimulation was due to a specific inability of TLR7 triggering to induce IFN in monocytes, we stimulated monocytes with GDQ and Loxo as TLR7 ligands, and with ssRNADR and PolyU as TLR8-specific ligands, and IFN gene expression was examined 16 hours later (Fig 8F). In agreement with our previous observations, GDQ and Loxo failed to induce IFN genes, while both ssRNADR and PolyU significantly increased the expression of *IFNA1*, *IFNA2* and *IFNB1*. Pre-treatment of monocytes with IRS661 and IRS957 confirmed the TLR8-specificity of the results obtained (Fig 8G).

Induction of a type I IFN response in APCs upon nucleic acid-sensing TLR stimulation can involve the activation of TBK1 by nucleic acid sensing TLRs(*65*). Subsequently, IRF3 and IRF7 are activated(*66, 67*) and both are important for the expression of type I IFN genes(*64*). We decided to examine the activation of the TBK1-IRF3/7 pathway in monocytes stimulated with IMQ or ssRNA40 as compared to vehicle-treated cells (Fig 8, H and I). TBK1 was significantly upregulated by ssRNA40 during the first 30 min of activation. In contrast, there was only a slight increase in the phosphorylation of TBK1 after IMQ stimulation at 15 min as compared to vehicle. We then examined the phosphorylation of IRF3 by TBK1 at Ser^{386} and while both TLR7 and TLR8 stimulation induced IRF3 activation, phosphorylation of IRF3 by ssRNA40 was significantly higher at each time point to that of IMQ-stimulated cells (Fig 8I).

TLR7-dependent Ca^{2+} signaling inhibits type I IFN response

The increased IRF3 activation by IMQ did not correlate with the lack of IFN gene expression, suggesting that other mechanisms could be inhibiting the expression of type I IFN genes. We hypothesized that a TLR7-specific pathway triggered by IMQ would inhibit IFN expression. An important difference we had previously observed between TLR7 and TLR8 signaling on $CD4^+$ T

cells was an increase in intracellular Ca^{2+} triggered by TLR7 stimulation that did not occur after ssRNA40 stimulation(*68*). As Ca^{2+} signaling has been involved in the phenotype of APC and it is an important modulator of cell responses during viral infections(*69, 70*), we decided to examine whether TLR7 stimulation induced an increase in intracellular Ca^{2+} concentration in monocytes (Fig 9A). Unlike ssRNA40, IMQ stimulation induced a significant increase in intracellular Ca^{2+} concentration in a dose-dependent manner (Fig 9A). The effect observed was TLR7-dependent, as pre-incubation with IRS661 almost completely inhibited Ca^{2+} flux as compared to IRS control-treated monocytes (Fig 9B). In order to determine the origin of the increase in Ca^{2+}, we stimulated monocytes with IMQ in the presence of EGTA (extracellular Ca^{2+} chelator) and xestopongin C, an inhibitor of inositol triphosphate (IP3)-dependent Ca^{2+} release. While chelation of extracellular Ca^{2+} did not affect IMQ-induced increase in Ca^{2+}, xestopongin C inhibited it almost completely, suggesting that TLR7-driven increased in intracellular Ca^{2+} occurs through depletion of internal stores located in the endoplasmic reticulum (Fig 9C).

We then hypothesized that TLR7-dependent Ca^{2+} flux would negatively affect the expression of type I IFN genes. To test this, we used Quin-2 AM as a chelating agent to block free intracellular Ca^{2+}(*68, 71*) and we stimulated monocytes with IMQ to examine the expression of type I IFN genes (Fig 9, D and E). While Quin-2 AM alone had no significant effect on the expression of any of the genes tested, stimulation of monocytes with IMQ in the presence of increasing concentrations of Quin-2 AM significantly upregulated the expression of *IFNA1* and *IFNA2*. Accordingly, the expression of ISGs was also upregulated by IMQ when Ca^{2+} was blocked (Fig 9D). The increased *IFNA* gene expression was confirmed at protein level by IFNα in the culture supernatant (Fig 9F). These results suggest that TLR7-dependent Ca^{2+} signaling inhibited IFNα secretion and type I IFN genes, although Ca^{2+} blockade had an uneven effect on IRF3 and IRF7 expression (Fig 9G). While monocyte stimulation with IMQ in the presence of Quin-2 AM

significantly upregulated the expression of IRF7 at 24 hours, IRF3 expression was significantly downregulated upon Ca^{2+} chelation as compared to IMQ only treated cells. These results were similar to the pattern of *IRF3* and *IRF7* expression observed upon TLR8 stimulation as compared to vehicle-treated cells at similar time points (fig S7). Taken together these results suggest that TLR7-dependent Ca^{2+} signaling acts as a negative regulator of type I IFN response in human $CD14^{+}$ monocytes.

TLR7-dependent FOSL1 expression is Ca^{2+}- and ERK-dependent.

We decided to explore further the mechanism by which TLR7 stimulation increased the expression of *FOSL1* (Fig 7). For this, we examined the involvement of the molecules previously identified that were specifically activated after TLR7 activation, including p38, ERK, JNK (Fig 6) and Ca^{2+} (Fig 8). We stimulated monocytes with IMQ in the presence of inhibitors of p38 (SB203580), ERK1/2 (SCH772984), JNK (SP600125), and the Ca^{2+} intracellular chelator Quin-2 AM, and we measured *FOSL1* expression (Fig 10). While p38 and JNK inhibition did not abrogate IMQ-dependent *FOSL1* upregulation, both ERK1/2 inhibition and Ca^{2+} chelation with Quin-2 AM significantly inhibited the expression of *FOSL1* after TLR7 stimulation, suggesting that both TLR7-dependent ERK1/2 activation and Ca^{2+} fluxes are necessary for *FOSL1* upregulation.

FOSL1 can act as a negative regulator of IFN signaling in vivo and in vitro(*72*), so we decided to examine whether TLR7-induced FOSL1 was partly responsible for the inhibition of type I IFN responses after IMQ stimulation (Fig 10E). FOSL1 silencing in monocytes did not restore IFNA expression after IMQ activation nor affected IFNA gene expression levels after ssRNA40 stimulation, suggesting that FOSL1 is not involved in the inhibition of type I IFN response after TLR7 stimulation.

Discussion

The innate immune system is armed with receptors that sense pathogens to mount effective immune responses during infection. Monocytes are a major target of many viruses, and infection not only induces monocyte differentiation into other cell populations, but it also activates them to perform effector functions(*4*). In this work we dissect the TLR7- and TLR8-dependent events that tune the activation of human monocytes upon RNA virus infection, and we define TLR7- and TLR8-specific signaling pathways in this process (fig S8). Furthermore, by dissecting the signaling pathway downstream TLR7 we define FOSL1 as a major regulator that inhibits the expression of type 1 cytokines upon TLR7 signaling. Finally, we describe the TLR7-Ca^{2+}axis as a negative regulator of type I IFN responses in $CD14^{+}$ monocytes.

While APCs in general utilize a variety of sensors to detect pathogens, initial virus sensing is carried out by RLRs leading to local IFN production(*11*). Subsequently, both RLR and TLR act in concert to specifically tune the adaptive immune response(*31*). Thus, while RLR signaling is essential for the initial triggering of antiviral responses, the TLR serve a secondary role to drive specific cytokine production and type I IFN responses to regulate and shape the type of adaptive immune response and programming of cell-mediated immunity(*73, 74*). In this regard, we observed that monocyte infection with a variety of RNA viruses led to various phenotypes that were dependent on TLR7 and/or TLR8 signaling. However, and in agreement with the involvement of RLR in innate immune activation, TLR7 or TLR8 blockade upon virus infection did not completely abrogate the expression of cytokines in our experimental system(*75, 76*). The concerted actions of these pathways to human monocyte function has not been addressed, and it will be interesting for future studies to examine the cross-talk between TLR7 and TLR8 signaling and other nucleic acid sensing pathways in human monocytes during virus infection.

Our data demonstrated that TLR7 and TLR8 signaling in $CD14^{+}$ monocytes are significantly different, and while TLR7 preferentially upregulated Th17-polarizing cytokines primarily through

the activation of MAPK cascades that lead to AP-1 activation, TLR8 predominantly induced type-1 cytokines, that are NFκB dependent. This observation is in agreement with previous works that suggested differential roles of TLR7 and TLR8 signaling in other immune cell populations, such as dendritic cells and neutrophils(*77-81*), and supports previous observations of preferential type 1 cytokine secretion upon TLR8 as compared to TLR7 stimulation(*77*), and inhibition of type 1 cytokines by TLR7 in other disease settings(*82*). Moreover, TLR7 engagement in DC leads to an activated phenotype with increase ability to promote Th17 responses in an in vivo model of uveitis(*83*) and in human DC in vitro(*84*). Intriguingly, FOSL1 is expressed primarily in Th17 cells as compared to other T helper subsets, and IL-17 is directly controlled by FOSL1(*85*). Moreover, FOSL1 expression is correlated with high psoriasis(*86*) and increased susceptibility to collagen-induced arthritis(*85*).

AP-1 family of transcription factors are essential molecules in mammalian cells that mediate the regulation of genes involved in proliferation, activation and other cell functions. The observation that FOSL1 inhibits type 1 pro-inflammatory cytokines underscores the complexity of the AP-1 family, which is generally overlooked, and raises the questions of whether individual stimuli activate specific AP-1 dimers, what the transcriptional targets for each dimer are, and what the distribution of AP-1 dimers across cells types or over time in a specific cell type are(*53*). Furthermore, in agreement with our results, other AP-1 members have been shown to perform inhibitory functions during TLR signaling(*87, 88*). For example, loss of cFOS in mice results in increased NFκB signaling in response to LPS(*89, 90*) and overexpression of FOSL1 in macrophages inhibits the expression of pro-inflammatory cytokines upon LPS stimulation(*91, 92*). We observed that the TLR7-dependent increase in *FOSL1* expression was dependent on both increased Ca^{2+} concentrations and ERK activation. Previous data have established the role of Ca^{2+} on ERK activation(*93, 94*) and therefore, it is plausible that these two events occur

sequentially after TLR7 activation to induce the expression of *FOSL1*, with TLR7-induced Ca^{2+} increase activating ERK, which in turn is required for the upregulation of *FOSL1*.

The observation that TLR7 ligation inhibits type I IFN response by inducing intracellular Ca^{2+} release in monocytes is unexpected and further investigations are warranted to dissect the mechanisms by which calcium modulates type I IFN responses. However, several works have suggested a negative relationship between calcium signaling and IFN activity(*95-97*), and it is well known that viruses utilize diverse strategies to inhibit type I IFN responses(*98*). It is thus tempting to speculate that RNA viruses would utilize TLR7 signaling when infecting $CD14^{+}$ monocytes to avoid type I IFN responses and expand in the host, be transported to other tissues, etc. In support of our data, several signaling molecules that are involved in TLR7 signaling in human monocytes have been shown to inhibit type I IFN responses in other cell types, such as MEK1/2-ERK(*99*) and FOSL1(*72*). Moreover, the absence of type I IFN expression upon TLR7 stimulation had previously been observed in human macrophages upon HCV infection(*14*) and in human dendritic cells upon Influenza infection or small molecule activation(*100*).

The involvement of nucleic acid-sensing mechanisms in the immune response against infections and even in autoimmune diseases(*101*), makes these pathways interesting targets for drug design. TLR agonists are being tested in clinical trials in cancer and infectious diseases, as they provide enhanced immune responses in these settings(*10, 102*). In this regard, our results have important consequences on the selection of these agonists as adjuvants in therapeutic immunizations against cancer or prophylactic vaccines against pathogens, and demonstrate that the fundamental differences in signaling between these two related receptors could potentially be harnessed to tailor specific immune responses in various disease settings.

Materials and Methods

Study Subjects

Peripheral blood was drawn from healthy individuals after informed consent and approval by the Institutional Review Board at Yale University and Imperial College London. All experiments were performed conformed to the principles set out in the WMA Declaration of Helsinki and the Department of Health and Human Services Belmont Report.

Cell Culture reagents

Cells were cultured in RPMI 1640 media supplemented with 2 nM L-glutamine, 5 mM HEPES, 100 U/μg/ml penicillin/streptomycin (Biowhittaker), 0.5 mM sodium pyruvate, 0.05 mM non-essential amino acids (Life Technologies), and 5% human AB serum (Gemini Bio-Products). Monocytes were cultured in 96-well polypropylene plates to avoid non-specific activation by adhesion to polystyrene.

The TLR7-specific inhibitory sequence IRS661, the TLR8-specific sequence IRS957 and a non-target sequence as a control were synthesized by Sigma on a phosphorothioate backbone and used at 2-5 μM. None of these inhibitory sequences induced significant cell death at the concentrations described above. The p38 inhibitor SB203580 (Selleckchem)(*103, 104*), the ERK1/2 inhibitor SCH772984 (Selleckchem)(*105, 106*) and the JNK inhibitor SP600125 (Invivogen)(*107, 108*) were used at 2 and 10 μM. The Ca^{2+} chelator Quin 2-AM (Thermo Scientific) was used at 0.5 μM and 2.5 μM(*68*).

Cell Isolation and activation with TLR ligands

Peripheral blood mononuclear cells (PBMC) were isolated from healthy donors by Ficoll-Paque PLUS gradient centrifugation (GE Healthcare). Classical $CD14^+$ monocytes were isolated by positive selection using the Easy Sep Human CD14 Positive Selection Kit (Stem Cell

Technologies). Total $CD4^+$ T cells were isolated by negative selection using the Easy Sep Human $CD4^+$ T-cell Enrichment kit (Stem Cell Technologies). B cell isolation was performed with the Easy Sep Human CD19 Positive selection kit II (Stem Cell Technologies). The following TLR ligands were used to stimulate $CD14^+$ monocytes: Imiquimod, in concentrations ranging from 0.1 to 10 μg/ml, ssRNA40/LyoVec (InvivoGen), in concentrations ranging from 0.1 to 5 μg/ml, 0.5 mM Loxoribine, 2.5 μg/ml Gardiquimod, 2.5 μg/ml ssRNA-DR and 2.5 μg/ml PolyU. All TLR ligands (<0.001 EU/μg; EndoFit) were obtained from InvivoGen and resuspended in endotoxin-free water according to the manufacturer's recommendations.

Monocyte – RNA virus co-cultures

$CD14^+$ monocytes were stimulated with RNA viruses at a multiplicity of infection (MOI) of 5 for 16 hours at 37°C. The viruses used in this manuscript are Coxsackievirus B1 (Conn-5 strain, CV), Measles virus (Edmonton strain, MV), Sendai virus (Sendai/52 strain, SV), Encephalomyocarditis virus (EMCV), all obtained from ATCC. Vesicular stomatitis virus (Indiana strain, VSV) was a kind gift from Dr. Akiko Iwasaki's laboratory (Department of Immunobiology, Yale School of Medicine) and Influenza A virus (PR8 strain, IAV) was a kind gift from Dr. Alfonso Garcia-Sastre's laboratory (Icahn School of Medicine, Mount Sinai, New York). Culture supernatant was collected for cytokine release measurement by ELISA and cells were lysed in RLT Plus buffer (QIAGEN) for gene expression assays.

$CD14^+$:$CD4^+$ T cell co-cultures

Freshly isolated $CD14^+$ monocytes were resuspended at 10^6 cells/ml in complete medium and stimulated with IMQ (2.5 μg/ml), ssRNA40 (2.5 μg/ml) or vehicle for 16 hours at 37°C. Subsequently, monocytes were co-cultured with isolated $CD4^+$ T cells from the same donor in the presence of anti-CD3 (UCHT1 clone, BD Biosciences, 1 μg/ml) at different T cell:monocyte ratios.

Supernatant was collected after 24, 72 and 120 hours for IFNγ and IL-17 measurement by ELISA, and the cells were stained with LIVE/DEAD fixable violet dye (Thermo Scientific), CD14 and CD3. $CD3^{+}CD14^{-}$ T cells were sorted on a FACS Aria (BD Biosciences) and lysed with RLT Plus buffer (QIAGEN) to examine gene expression by real-time PCR.

Enzyme-linked immunosorbent assay (ELISA)

IL-1β, IL-6, IL-12, IL-27, and TNFα were measured from supernatants of stimulated monocyte cultures, and IL-17 and IFN-γ from supernatants of monocyte:$CD4^{+}$ T cell co-culture experiments with Human DuoSet ELISA kits from R&D Systems, according to manufacturer's recommendations.

IFN-α and IFN-β were measured from stimulated monocyte cultures using the VeriKine Human ELISA kits for IFN-α and IFNβ respectively (PBL assay science), using manufacturer's recommendations.

Quantification of mRNA expression levels by real-time PCR

RNA was isolated using the QIAGEN RNeasy Micro Kit (QIAGEN), or the ZR-96 Quick RNA (Zymo Research, Irvine, CA) following manufacturer′s guidelines and converted to cDNA by reverse transcription (RT) with random hexamers and Multiscribe RT (TaqMan Reverse Transcription Reagents; ThermoFisher Scientific). For mRNA gene expression assays, probes were obtained from Life ThermoFisher Scientific and the reactions were set up following manufacturer's guidelines and run on a StepOnePlus Real-Time PCR System (ThermoFisher Scientific). Values are represented as the difference in Ct values normalized to β2-microglobulin for each sample as per the following formula: Relative RNA expression = $(2^{-\Delta Ct}) \times 1000$.

For mRNA expression assays, the following probes were used: *ATF1* Hs00909673_m1, *ATF2* Hs01095345_m1, *ATF3* Hs00231069_m1, *ATF4* Hs00909569_g1, *ATF5* Hs01119208_m1, *ATF6* Hs00232586_m1, *ATF7* Hs00232499_m1, *B2M* Hs00187842_m1, *BST2* Hs00171632_m1, *CCL20* Hs00171125_m1, *CD40* Hs01002913_g1, *CD74* Hs00269961_m1, *CFOS* Hs04194186_s1, *CXCL10* Hs00171042_m1, *CXCL8* Hs99999034_m1, *EBI3* Hs01057148_m1, *EIF2AK2* Hs00169345_m1, *FOS* Hs04194186_s1, *FosB* Hs00171851_m1, *FOSL1* Hs04187685_m1, *FOSL2* Hs01050117_m1, *FOXP3* Hs01085834_m1, *GATA3* Hs00231122_m1, *GZMB* Hs01554355_m1, *ICOSLG* Hs00323621_m1, *IFITM1* Hs00705137_s1, *IFITM2* Hs00829485_sH, *IFNA1* Hs00855471_g1, *IFNA2* Hs00265051_s1, *IFNB1* Hs01077958_s1, *IFNG* Hs00989291_m1, *IL10* Hs001174086_m1, *IL12B* Hs01011519_m1, *IL1B* Hs99999029_m1, *IL17A* Hs00174383_m1, *IL21* Hs00222327_m1, *IL23A* Hs00372324_m1, *IL27* Hs00377366_m1, *IL4* Hs00174122_m1, *IL6* Hs00174131_m1, *IRF1* Hs009171965_m1, *IRF3* Hs01547283_m1, *IRF5* Hs00158114_m1, *IRF7* Hs00185375_m1, *IRF9* Hs00196051_m1, *ISG15* Hs00192713_m1, *JDP2* Hs00185689_m1, *JUN* Hs01103582_s1, *JUNB* Hs00357891_s1, *JUND* Hs04187679_s1, *MOV10* Hs00253093_m1, *MX2* Hs01550808_m1, *RORC* Hs01076122_m1, *TBX21* Hs00203436_m1, *TGFB1* Hs00998133_m1, *TLR1* Hs00413978_m1, *TLR2* Hs01014511_m1, *TLR3* Hs01551078_m1, *TLR4* Hs00152939_m1, *TLR5* Hs00152825_m1, *TLR6* Hs00271977_m1, *TLR7* Hs00152971_m1, *TLR8* Hs00152972_m1, *TLR9* Hs00152973_m1, *TLR10* Hs01675179_m1, *TNF* Hs00174128_m1, *TREX1* Hs03989617_s1, *TRIM5* Hs01552559_m1.

Analysis of phosphorylation by flow cytometry

Isolated monocytes were left at 37°C overnight in complete medium to rest before phosphorylation assays. Cells were stimulated with 5 μg/ml IMQ or 5 μg/ml ssRNA40 and fixed at various time points with Fixation buffer (BD Biosciences), permeabilized with Perm III buffer (BD Biosciences)

according to manufacturer's instructions and stained with anti-human phospho-p38 (Thr^{180}/Tyr^{182}), phospho-MEK1/2 (Ser^{218}/Ser^{222}), phospho-ERK1/2 (Thr^{202}/Tyr^{204}), phospho-p65 (Ser^{529}) and phospho-TBK1 (Ser^{172}) from BD Biosciences and anti-human phospho-MKK3/6 (Ser^{218}), phospho-MKK4/7 (Ser^{271}/Thr^{275}) and phospho-IRF3 (Ser^{386}) from Bioss antibodies. Samples were run on a BD Fortessa cytometer and data were analyzed using FlowJo software (TreeStar).

Extra- and intracellular protein staining

For extracellular staining, monocytes were stimulated with 5 μg/ml IMQ or 5 μg/ml ssRNA40 for 12 hours and CD40 and ICOSL were detected with anti-human CD40 (Clone 5C3) and anti-human ICOSL (clone 2D3), from Biolegend. For intracellular staining, monocytes were stimulated as above in the presence of GolgiStop (BD Biosciences) for 8 hours at 37°C. For both extra- and intracellular stainings LIVE/DEAD viability dye was used to exclude dead cells before antibody staining, and a subsequent FcR blocking step (FcR blocking reagent, human, Miltenyi Biotec) was performed before fixation and the addition of antibodies. Cells were fixed using the Foxp3 staining buffers (Thermo Scientific) following manufacturer's recommendations. For intracellular cytokine staining, the following anti-human antibodies were used: IL-1β (clone AS10), IL-12 (clone C11.5), TNFα (clone Mab11) from BD Biosciences, and IL-23 p19 (clone 23dcdp) from eBioscience. Samples were run on a BD Fortessa instrument and analyzed with FlowJo software.

Gene silencing by siRNA

Gene silencing on $CD14^+$ monocytes was performed as previously published(*109*) with some modifications. Briefly, monocytes were resuspended at 1.5 $x10^6$ cells/ml in complete medium and transfected with 200 mM siRNA (siGENOME SMARTpool, Dharmacon) for *TLR7*, *TLR8*, *ATF1*, *ATF2*, *FOSL1* or *FOSL2* using HiPerFect (QIAGEN). 1.5 days after transfection, some cells were lysed to confirm target gene silencing and the rest of monocytes were harvested, plated at 5 x

10^4 cells/well in 96 well plates and stimulated with IMQ or ssRNA40 at 5 μg/ml for 16 hours. Supernatant was collected for ELISA determination of cytokines and cells were lysed with RLT Plus buffer (QIAGEN) for gene expression analysis.

Measurement of intracellular calcium

Monocytes were labeled ex vivo with 5 μM Indo-1 AM (Thermo Scientific) in PBS for 45 min at 37°C. Cells were washed to remove excess of Indo-1 AM, resuspended at 10^6 cells/ml in PBS and rested for 30 min at 37°C. When necessary, IRS661 or IRS control were added at 2.5 μM during the 30 min of resting. Xestopongin C (Sigma-Aldrich) and EGTA were added during the 30 min of resting at 1μM(*110, 111*) and 2 mM(*112*), respectively. The samples were acquired on a BD Fortessa for approximately 2 minutes initially to determine basal levels of Ca^{2+}. Subsequently, IMQ, ssRNA40 or ionomycin were added to the cells at the appropriate concentrations. Samples were acquired for approximately 8 more minutes to determine the increase in intracellular Ca^{2+} concentration. Data were analyzed with FlowJo software.

Statistical analysis

GraphPad Prism software was used for statistical analysis. A paired two-tailed t-test was used to determine significant differences in the means of two groups. One- or two-tailed analysis of variance (ANOVA) with correction for multiple comparisons (see Figure legends for specifics) for analysis of more than two groups. Unless otherwise specified, data are represented as mean ± s.e.m. P values of 0.05 or less were considered significant.

Supplementary Materials

Fig S1. Expression of TLR7 and TLR8 by human $CD14^+$ monocytes.

Fig S2. TLR7 and TLR8 blockade and virus infection.

Fig S3. Cytokine expression by TLR7- and TLR8-silenced monocytes after RNA virus infection.

Fig S4. Type I IFN response by TLR7- and TLR8-silenced monocytes after RNA virus infection.

Fig S5. Th1- and Th17-polarizing phenotype after TLR7 and TLR8 activation in human monocytes.

Fig S6. Redundant roles of ATF1, ATF2 and FOSL2 in inducing Th17-type cytokines after TLR7 stimulation.

Fig S7. Kinetics of IRF3 and IRF7 expression after TLR7 and TLR8 stimulation.

Fig S8. Schematic of TLR7 and TLR8 signaling in human $CD14^+$ monocytes.

References and Notes

1. L. Ziegler-Heitbrock *et al.*, Nomenclature of monocytes and dendritic cells in blood. *Blood* **116**, e74-80 (2010).
2. K. L. Wong *et al.*, Gene expression profiling reveals the defining features of the classical, intermediate, and nonclassical human monocyte subsets. *Blood* **118**, e16-31 (2011).
3. A. C. Villani *et al.*, Single-cell RNA-seq reveals new types of human blood dendritic cells, monocytes, and progenitors. *Science (New York, N.Y.)* **356**, (2017).
4. N. V. Serbina, T. Jia, T. M. Hohl, E. G. Pamer, Monocyte-mediated defense against microbial pathogens. *Annu Rev Immunol* **26**, 421-452 (2008).
5. M. F. de Castro-Amarante *et al.*, Human T Cell Leukemia Virus Type 1 Infection of the Three Monocyte Subsets Contributes to Viral Burden in Humans. *J Virol* **90**, 2195-2207 (2015).
6. D. Michlmayr, P. Andrade, K. Gonzalez, A. Balmaseda, E. Harris, CD14(+)CD16(+) monocytes are the main target of Zika virus infection in peripheral blood mononuclear cells in a paediatric study in Nicaragua. *Nat Microbiol* **2**, 1462-1470 (2017).

7. F. Perdomo-Celis, D. M. Salgado, C. F. Narvaez, Magnitude of viremia, antigenemia and infection of circulating monocytes in children with mild and severe dengue. *Acta Trop* **167**, 1-8 (2017).

8. M. Savard *et al.*, Infection of primary human monocytes by Epstein-Barr virus. *J Virol* **74**, 2612-2619 (2000).

9. Z. Her *et al.*, Active infection of human blood monocytes by Chikungunya virus triggers an innate immune response. *Journal of immunology* **184**, 5903-5913 (2010).

10. T. Junt, W. Barchet, Translating nucleic acid-sensing pathways into therapies. *Nat Rev Immunol* **15**, 529-544 (2015).

11. Y. M. Loo, M. Gale, Jr., Immune signaling by RIG-I-like receptors. *Immunity* **34**, 680-692 (2011).

12. F. Heil *et al.*, Species-specific recognition of single-stranded RNA via toll-like receptor 7 and 8. *Science (New York, N.Y.)* **303**, 1526-1529 (2004).

13. T. U. Metcalf *et al.*, Human Monocyte Subsets Are Transcriptionally and Functionally Altered in Aging in Response to Pattern Recognition Receptor Agonists. *Journal of immunology* **199**, 1405-1417 (2017).

14. M. A. Chattergoon *et al.*, HIV and HCV activate the inflammasome in monocytes and macrophages via endosomal Toll-like receptors without induction of type 1 interferon. *PLoS Pathog* **10**, e1004082 (2014).

15. T. Eigenbrod, K. Pelka, E. Latz, B. Kreikemeyer, A. H. Dalpke, TLR8 Senses Bacterial RNA in Human Monocytes and Plays a Nonredundant Role for Recognition of Streptococcus pyogenes. *Journal of immunology* **195**, 1092-1099 (2015).

16. R. Firdaus *et al.*, Modulation of TLR 3, 7 and 8 expressions in HCV genotype 3 infected individuals: potential correlations of pathogenesis and spontaneous clearance. *Biomed Res Int* **2014**, 491064 (2014).

17. R. T. Lester *et al.*, Toll-like receptor expression and responsiveness are increased in viraemic HIV-1 infection. *Aids* **22**, 685-694 (2008).

18. W. Hou *et al.*, Viral infection triggers rapid differentiation of human blood monocytes into dendritic cells. *Blood* **119**, 3128-3131 (2012).

19. E. K. Alidjinou *et al.*, Monocytes of Patients with Type 1 Diabetes Harbour Enterovirus RNA. *Eur J Clin Invest* **45**, 918-924 (2015).

20. M. A. Benkahla *et al.*, Coxsackievirus-B4E2 can infect monocytes and macrophages in vitro and in vivo. *Virology* **522**, 271-280 (2018).

21. M. S. Oberste *et al.*, Human febrile illness caused by encephalomyocarditis virus infection, Peru. *Emerg Infect Dis* **15**, 640-646 (2009).

22. R. B. Tesh, The prevalence of encephalomyocarditis virus neutralizing antibodies among various human populations. *Am J Trop Med Hyg* **27**, 144-149 (1978).

23. P. S. Pillai *et al.*, Mx1 reveals innate pathways to antiviral resistance and lethal influenza disease. *Science (New York, N.Y.)* **352**, 463-466 (2016).

24. T. Ronni, T. Sareneva, J. Pirhonen, I. Julkunen, Activation of IFN-alpha, IFN-gamma, MxA, and IFN regulatory factor 1 genes in influenza A virus-infected human peripheral blood mononuclear cells. *Journal of immunology* **154**, 2764-2774 (1995).

25. L. M. Esolen, B. J. Ward, T. R. Moench, D. E. Griffin, Infection of monocytes during measles. *J Infect Dis* **168**, 47-52 (1993).

26. J. Pirhonen, T. Sareneva, M. Kurimoto, I. Julkunen, S. Matikainen, Virus infection activates IL-1 beta and IL-18 production in human macrophages by a caspase-1-dependent pathway. *Journal of immunology* **162**, 7322-7329 (1999).

27. J. Siren *et al.*, Cytokine and contact-dependent activation of natural killer cells by influenza A or Sendai virus-infected macrophages. *J Gen Virol* **85**, 2357-2364 (2004).

28. D. Bussfeld, M. Nain, P. Hofmann, D. Gemsa, H. Sprenger, Selective induction of the monocyte-attracting chemokines MCP-1 and IP-10 in vesicular stomatitis virus-infected human monocytes. *J Interferon Cytokine Res* **20**, 615-621 (2000).

29. T. Tomczyk *et al.*, Immune Consequences of in vitro Infection of Human Peripheral Blood Leukocytes with Vesicular Stomatitis Virus. *J Innate Immun* **10**, 131-144 (2018).

30. S. Jensen, A. R. Thomsen, Sensing of RNA viruses: a review of innate immune receptors involved in recognizing RNA virus invasion. *J Virol* **86**, 2900-2910 (2012).

31. A. Iwasaki, A virological view of innate immune recognition. *Annu Rev Microbiol* **66**, 177-196 (2012).

32. J. L. Cervantes, B. Weinerman, C. Basole, J. C. Salazar, TLR8: the forgotten relative revindicated. *Cell Mol Immunol* **9**, 434-438 (2012).

33. J. Cros *et al.*, Human CD14dim monocytes patrol and sense nucleic acids and viruses via TLR7 and TLR8 receptors. *Immunity* **33**, 375-386 (2010).

34. R. D. Pawar *et al.*, Inhibition of Toll-like receptor-7 (TLR-7) or TLR-7 plus TLR-9 attenuates glomerulonephritis and lung injury in experimental lupus. *J Am Soc Nephrol* **18**, 1721-1731 (2007).

35. J. Hurst *et al.*, TLR7 and TLR8 ligands and antiphospholipid antibodies show synergistic effects on the induction of IL-1beta and caspase-1 in monocytes and dendritic cells. *Immunobiology* **214**, 683-691 (2009).

36. J. L. Cervantes *et al.*, Phagosomal signaling by Borrelia burgdorferi in human monocytes involves Toll-like receptor (TLR) 2 and TLR8 cooperativity and TLR8-mediated induction of IFN-beta. *Proc Natl Acad Sci U S A* **108**, 3683-3688 (2011).

37. C. M. Paulos *et al.*, The inducible costimulator (ICOS) is critical for the development of human T(H)17 cells. *Sci Transl Med* **2**, 55ra78 (2010).

38. E. Stuber, W. Strober, M. Neurath, Blocking the CD40L-CD40 interaction in vivo specifically prevents the priming of T helper 1 cells through the inhibition of interleukin 12 secretion. *The Journal of experimental medicine* **183**, 693-698 (1996).

39. E. V. Acosta-Rodriguez *et al.*, Surface phenotype and antigenic specificity of human interleukin 17-producing T helper memory cells. *Nature immunology* **8**, 639-646 (2007).

40. F. Sallusto, D. Lenig, C. R. Mackay, A. Lanzavecchia, Flexible programs of chemokine receptor expression on human polarized T helper 1 and 2 lymphocytes. *The Journal of experimental medicine* **187**, 875-883 (1998).

41. T. Kawasaki, T. Kawai, Toll-Like Receptor Signaling Pathways. *Frontiers in Immunology* **5**, (2014).

42. T. D. Troutman, J. F. Bazan, C. Pasare, Toll-like receptors, signaling adapters and regulation of the pro-inflammatory response by PI3K. *Cell Cycle* **11**, 3559-3567 (2012).

43. M. J. Fenton, Review: transcriptional and post-transcriptional regulation of interleukin 1 gene expression. *International journal of immunopharmacology* **14**, 401-411 (1992).

44. W. Liu *et al.*, AP-1 activated by toll-like receptors regulates expression of IL-23 p19. *The Journal of biological chemistry* **284**, 24006-24016 (2009).

45. T. Lawrence, The nuclear factor NF-kappaB pathway in inflammation. *Cold Spring Harb Perspect Biol* **1**, a001651 (2009).

46. Q. Zhang, M. J. Lenardo, D. Baltimore, 30 Years of NF-kappaB: A Blossoming of Relevance to Human Pathobiology. *Cell* **168**, 37-57 (2017).

47. M. A. Collart, P. Baeuerle, P. Vassalli, Regulation of tumor necrosis factor alpha transcription in macrophages: involvement of four kappa B-like motifs and of constitutive and inducible forms of NF-kappa B. *Mol Cell Biol* **10**, 1498-1506 (1990).

48. A. N. Shakhov, M. A. Collart, P. Vassalli, S. A. Nedospasov, C. V. Jongeneel, Kappa B-type enhancers are involved in lipopolysaccharide-mediated transcriptional activation of

the tumor necrosis factor alpha gene in primary macrophages. *The Journal of experimental medicine* **171**, 35-47 (1990).

49. T. L. Murphy, M. G. Cleveland, P. Kulesza, J. Magram, K. M. Murphy, Regulation of interleukin 12 p40 expression through an NF-kappa B half-site. *Mol Cell Biol* **15**, 5258-5267 (1995).

50. J. Liu, X. Guan, X. Ma, Regulation of IL-27 p28 gene expression in macrophages through MyD88- and interferon-gamma-mediated pathways. *The Journal of experimental medicine* **204**, 141-152 (2007).

51. M. A. Poleganov, M. Bachmann, J. Pfeilschifter, H. Muhl, Genome-wide analysis displays marked induction of EBI3/IL-27B in IL-18-activated AML-derived KG1 cells: critical role of two kappaB binding sites in the human EBI3 promotor. *Mol Immunol* **45**, 2869-2880 (2008).

52. E. Shaulian, AP-1--The Jun proteins: Oncogenes or tumor suppressors in disguise? *Cell Signal* **22**, 894-899 (2010).

53. J. Hess, P. Angel, M. Schorpp-Kistner, AP-1 subunits: quarrel and harmony among siblings. *J Cell Sci* **117**, 5965-5973 (2004).

54. M. R. Young, N. H. Colburn, Fra-1 a target for cancer prevention or intervention. *Gene* **379**, 1-11 (2006).

55. T. Suzuki *et al.*, Difference in transcriptional regulatory function between c-Fos and Fra-2. *Nucleic Acids Res* **19**, 5537-5542 (1991).

56. K. Yoshioka, T. Deng, M. Cavigelli, M. Karin, Antitumor promotion by phenolic antioxidants: inhibition of AP-1 activity through induction of Fra expression. *Proc Natl Acad Sci U S A* **92**, 4972-4976 (1995).

57. A. E. Abdalla, Q. Li, L. Xie, J. Xie, Biology of IL-27 and its role in the host immunity against Mycobacterium tuberculosis. *Int J Biol Sci* **11**, 168-175 (2015).

58. Y. Fu *et al.*, Regulation of tumor necrosis factor alpha promoter by human parvovirus B19 NS1 through activation of AP-1 and AP-2. *J Virol* **76**, 5395-5403 (2002).

59. Y. M. Kim, J. Y. Im, S. H. Han, H. S. Kang, I. Choi, IFN-gamma up-regulates IL-18 gene expression via IFN consensus sequence-binding protein and activator protein-1 elements in macrophages. *Journal of immunology* **165**, 3198-3205 (2000).

60. J. Liu *et al.*, Interleukin-12: an update on its immunological activities, signaling and regulation of gene expression. *Curr Immunol Rev* **1**, 119-137 (2005).

61. C. L. Newell, A. B. Deisseroth, G. Lopez-Berestein, Interaction of nuclear proteins with an AP-1/CRE-like promoter sequence in the human TNF-alpha gene. *J Leukoc Biol* **56**, 27-35 (1994).

62. Y. Tone *et al.*, Structure and chromosomal location of the mouse interleukin-12 p35 and p40 subunit genes. *European journal of immunology* **26**, 1222-1227 (1996).

63. J. Zhang *et al.*, Transcriptional suppression of IL-27 production by Mycobacterium tuberculosis-activated p38 MAPK via inhibition of AP-1 binding. *Journal of immunology* **186**, 5885-5895 (2011).

64. F. McNab, K. Mayer-Barber, A. Sher, A. Wack, A. O'Garra, Type I interferons in infectious disease. *Nat Rev Immunol* **15**, 87-103 (2015).

65. G. Oganesyan *et al.*, Critical role of TRAF3 in the Toll-like receptor-dependent and -independent antiviral response. *Nature* **439**, 208-211 (2006).

66. K. A. Fitzgerald *et al.*, IKKepsilon and TBK1 are essential components of the IRF3 signaling pathway. *Nature immunology* **4**, 491-496 (2003).

67. S. Sharma *et al.*, Triggering the interferon antiviral response through an IKK-related pathway. *Science (New York, N.Y.)* **300**, 1148-1151 (2003).

68. M. Dominguez-Villar, A. S. Gautron, M. de Marcken, M. J. Keller, D. A. Hafler, TLR7 induces anergy in human CD4(+) T cells. *Nature immunology* **16**, 118-128 (2015).

69. S. Hover, B. Foster, J. N. Barr, J. Mankouri, Viral dependence on cellular ion channels - an emerging anti-viral target? *J Gen Virol* **98**, 345-351 (2017).

70. Y. Zhou, T. K. Frey, J. J. Yang, Viral calciomics: interplays between Ca2+ and virus. *Cell Calcium* **46**, 1-17 (2009).

71. M. Bigby, P. Wang, J. F. Fierro, M. S. Sy, Phorbol myristate acetate-induced down-modulation of CD4 is dependent on calmodulin and intracellular calcium. *Journal of immunology* **144**, 3111-3116 (1990).

72. B. Cai, J. Wu, X. Yu, X. Z. Su, R. F. Wang, FOSL1 Inhibits Type I Interferon Responses to Malaria and Viral Infections by Blocking TBK1 and TRAF3/TRIF Interactions. *MBio* **8**, (2017).

73. S. Daffis, M. S. Suthar, K. J. Szretter, M. Gale, Jr., M. S. Diamond, Induction of IFN-beta and the innate antiviral response in myeloid cells occurs through an IPS-1-dependent signal that does not require IRF-3 and IRF-7. *PLoS Pathog* **5**, e1000607 (2009).

74. M. S. Suthar *et al.*, IPS-1 is essential for the control of West Nile virus infection and immunity. *PLoS Pathog* **6**, e1000757 (2010).

75. Y. M. Loo *et al.*, Distinct RIG-I and MDA5 signaling by RNA viruses in innate immunity. *J Virol* **82**, 335-345 (2008).

76. Z. Ma, B. Damania, The cGAS-STING Defense Pathway and Its Counteraction by Viruses. *Cell Host Microbe* **19**, 150-158 (2016).

77. K. S. Gorski *et al.*, Distinct indirect pathways govern human NK-cell activation by TLR-7 and TLR-8 agonists. *International immunology* **18**, 1115-1126 (2006).

78. B. Bergstrom *et al.*, TLR8 Senses Staphylococcus aureus RNA in Human Primary Monocytes and Macrophages and Induces IFN-beta Production via a TAK1-IKKbeta-IRF5 Signaling Pathway. *Journal of immunology* **195**, 1100-1111 (2015).

79. K. B. Gorden *et al.*, Synthetic TLR agonists reveal functional differences between human TLR7 and TLR8. *Journal of immunology* **174**, 1259-1268 (2005).

80. A. Larange, D. Antonios, M. Pallardy, S. Kerdine-Romer, TLR7 and TLR8 agonists trigger different signaling pathways for human dendritic cell maturation. *J Leukoc Biol* **85**, 673-683 (2009).

81. K. Makni-Maalej *et al.*, TLR8, but not TLR7, induces the priming of the NADPH oxidase activation in human neutrophils. *J Leukoc Biol* **97**, 1081-1087 (2015).

82. M. Salagianni *et al.*, Toll-like receptor 7 protects from atherosclerosis by constraining "inflammatory" macrophage activation. *Circulation* **126**, 952-962 (2012).

83. Q. Xiao *et al.*, TLR7 Engagement on Dendritic Cells Enhances Autoreactive Th17 Responses via Activation of ERK. *Journal of immunology* **197**, 3820-3830 (2016).

84. C. F. Yu *et al.*, Human plasmacytoid dendritic cells support Th17 cell effector function in response to TLR7 ligation. *Journal of immunology* **184**, 1159-1167 (2010).

85. Y. M. Moon *et al.*, The Fos-Related Antigen 1-JUNB/Activator Protein 1 Transcription Complex, a Downstream Target of Signal Transducer and Activator of Transcription 3, Induces T Helper 17 Differentiation and Promotes Experimental Autoimmune Arthritis. *Front Immunol* **8**, 1793 (2017).

86. V. V. Sobolev *et al.*, Effects of expression of transcriptional factor AP-1 FOSL1 gene on psoriatic process. *Bull Exp Biol Med* **150**, 632-634 (2011).

87. S. Dillon *et al.*, A Toll-like receptor 2 ligand stimulates Th2 responses in vivo, via induction of extracellular signal-regulated kinase mitogen-activated protein kinase and c-Fos in dendritic cells. *Journal of immunology* **172**, 4733-4743 (2004).

88. T. Kim *et al.*, Downregulation of lipopolysaccharide response in Drosophila by negative crosstalk between the AP1 and NF-kappaB signaling modules. *Nature immunology* **6**, 211-218 (2005).

89. S. Fujioka *et al.*, NF-kappaB and AP-1 connection: mechanism of NF-kappaB-dependent regulation of AP-1 activity. *Mol Cell Biol* **24**, 7806-7819 (2004).

90. N. Ray *et al.*, c-Fos suppresses systemic inflammatory response to endotoxin. *International immunology* **18**, 671-677 (2006).

91. K. Maruyama, G. Sano, N. Ray, Y. Takada, K. Matsuo, c-Fos-deficient mice are susceptible to Salmonella enterica serovar Typhimurium infection. *Infect Immun* **75**, 1520-1523 (2007).

92. H. Morishita *et al.*, Fra-1 negatively regulates lipopolysaccharide-mediated inflammatory responses. *International immunology* **21**, 457-465 (2009).

93. P. A. Atherfold, M. S. Norris, P. J. Robinson, E. W. Gelfand, R. A. Franklin, Calcium-induced ERK activation in human T lymphocytes. *Mol Immunol* **36**, 543-549 (1999).

94. J. M. Schmitt, G. A. Wayman, N. Nozaki, T. R. Soderling, Calcium activation of ERK mediated by calmodulin kinase I. *The Journal of biological chemistry* **279**, 24064-24072 (2004).

95. E. Genot, G. Bismuth, L. Degos, F. Sigaux, J. Wietzerbin, Interferon-alpha downregulates the abnormal intracytoplasmic free calcium concentration of tumor cells in hairy cell leukemia. *Blood* **80**, 2060-2065 (1992).

96. L. Wang *et al.*, Indirect inhibition of Toll-like receptor and type I interferon responses by ITAM-coupled receptors and integrins. *Immunity* **32**, 518-530 (2010).

97. C. Yue, J. Soboloff, A. M. Gamero, Control of type I interferon-induced cell death by Orai1-mediated calcium entry in T cells. *The Journal of biological chemistry* **287**, 3207-3216 (2012).

98. A. Garcia-Sastre, Ten Strategies of Interferon Evasion by Viruses. *Cell Host Microbe* **22**, 176-184 (2017).

99. V. Janovec *et al.*, The MEK1/2-ERK Pathway Inhibits Type I IFN Production in Plasmacytoid Dendritic Cells. *Front Immunol* **9**, 364 (2018).

100. J. Di Domizio *et al.*, TLR7 stimulation in human plasmacytoid dendritic cells leads to the induction of early IFN-inducible genes in the absence of type I IFN. *Blood* **114**, 1794-1802 (2009).

101. T. Celhar, A. M. Fairhurst, Toll-like receptors in systemic lupus erythematosus: potential for personalized treatment. *Front Pharmacol* **5**, 265 (2014).

102. M. P. Schon, M. Schon, TLR7 and TLR8 as targets in cancer therapy. *Oncogene* **27**, 190-199 (2008).

103. T. Davis *et al.*, Synthesis and in vivo activity of MK2 and MK2 substrate-selective p38alpha(MAPK) inhibitors in Werner syndrome cells. *Bioorg Med Chem Lett* **17**, 6832-6835 (2007).

104. C. Zhong, X. H. Liu, J. Chang, J. M. Yu, X. Sun, Inhibitory effect of resveratrol dimerized derivatives on nitric oxide production in lipopolysaccharide-induced RAW 264.7 cells. *Bioorg Med Chem Lett* **23**, 4413-4418 (2013).

105. Y. Li *et al.*, Long-term neurocognitive dysfunction in offspring via NGF/ ERK/CREB signaling pathway caused by ketamine exposure during the second trimester of pregnancy in rats. *Oncotarget* **8**, 30956-30970 (2017).

106. C. Ning *et al.*, Targeting ERK enhances the cytotoxic effect of the novel PI3K and mTOR dual inhibitor VS-5584 in preclinical models of pancreatic cancer. *Oncotarget* **8**, 44295-44311 (2017).

107. D. O. Moon *et al.*, JNK inhibitor SP600125 promotes the formation of polymerized tubulin, leading to G2/M phase arrest, endoreduplication, and delayed apoptosis. *Exp Mol Med* **41**, 665-677 (2009).

108. D. Vaishnav, P. Jambal, J. E. Reusch, S. Pugazhenthi, SP600125, an inhibitor of c-jun N-terminal kinase, activates CREB by a p38 MAPK-mediated pathway. *Biochemical and biophysical research communications* **307**, 855-860 (2003).

109. A. Troegeler *et al.*, An efficient siRNA-mediated gene silencing in primary human monocytes, dendritic cells and macrophages. *Immunol Cell Biol* **92**, 699-708 (2014).

110. M. Magnone *et al.*, Abscisic acid released by human monocytes activates monocytes and vascular smooth muscle cell responses involved in atherogenesis. *The Journal of biological chemistry* **284**, 17808-17818 (2009).

111. D. O. Moon *et al.*, Xestospongin C induces monocytic differentiation of HL60 cells through activation of the ERK pathway. *Food Chem Toxicol* **55**, 505-512 (2013).

112. S. K. Heo *et al.*, HVEM signaling in monocytes is mediated by intracellular calcium mobilization. *Journal of immunology* **179**, 6305-6310 (2007).

Acknowledgements: The authors would like to thank Prof Chris Cotsapas for critical review of the statistical methods used in this manuscript and Prof Akiko Iwasaki's laboratory and Prof Alfonso Garcia-Sastre's laboratory for providing reagents. **Author contributions:** M.D.M. designed and performed experiments, analyzed data and wrote the manuscript, K.D. performed experiments, A.C.D. performed and analyzed experiments, A.S.G. performed and analyzed experiments, M.D.V. designed and supervised the work, performed experiments, analyzed data and wrote the manuscript. **Competing interests:** The authors declare that they have no competing interests to declare**. Data and materials availability:** all data needed to evaluate the conclusions in the paper are present in the manuscript or the Supplementary materials.

Figure legends

Figure 1. RNA virus infections induce virus-specific cytokine and type I IFN responses by CD14$^+$ monocytes. **(A** to **D)** Human CD14$^+$ monocytes were stimulated ex vivo with Coxsackievirus (CV), Encephalomyocarditis virus (EMCV), Influenza A virus (IAV), Measles virus (MV), Sendai virus (SV) and Vesicular Stomatitis virus (VSV) at a MOI of 5 for 16 hours. (**A**) qRT-PCR analysis of Th1-type (left) and Th17-type (right) pro-inflammatory cytokine mRNA expression in virus exposed monocytes. (**B**) Pro-inflammatory cytokine secretion measured by ELISA. (**C**) qRT-PCR analysis of type I IFN response mRNA expression. (**D**) ELISA measurement of IFNα and IFNβ secretion in the culture supernatant. Gene expression data in **A** and **C** were arranged in a heatmap to identify virus-specific cytokine expression patterns. Colors are assigned using linear conditional formatting based on relative expression values of each gene for each donor and virus infection as compared to the expression value of that gene for all other donors and virus infections. Red denotes hig expression and blue low expression. *p<0.05, **p<0.005, ***p<0.001 by one-way ANOVA with Dunnett post-hoc test to correct for multiple comparisons (**B** and **D**). Data are heat maps (**A** and **C**) or means ± SEM (**B** and **D**) of 4 independent experiments with a total of 6 donors.

Figure 2. RNA virus infections induce different TLR7- and TLR8-specific cytokine expression pattern.. (**A** and **B**). Human CD14$^+$ monocytes were incubated ex vivo for 30 min with IRS661 or IRS957 and subsequently stimulated with Coxsackievirus (CV), Encephalomyocarditis virus (EMCV), Influenza A virus (IAV), Measles virus (MV), Sendai virus (SV) and Vesicular Stomatitis virus (VSV) at a MOI = 5 for 16 hours. (**A**) qRT-PCR analysis of Th17-type (left) and Th1-type (right) pro-inflammatory cytokine mRNA expression. (**B**) Cytokine secretion measured by ELISA. * p<0.05, ** p<0.005 (one-way ANOVA with Dunnett post-hoc test

to correct for multiple comparisons). Data are the mean ± SEM of 5 independent experiments with 2 donors in each.

Figure 3. RNA virus infections induce different TLR7- and TLR8-specific type I IFN gene expression patterns. (**A** to **C**). Human $CD14^+$ monocytes were incubated ex vivo for 30 min with IRS661 or IRS957 and subsequently stimulated with Coxsackievirus (CV), Encephalomyocarditis virus (EMCV), Influenza A virus (IAV), Measles virus (MV), Sendai virus (SV) and Vesicular Stomatitis virus (VSV) at a MOI = 5 for 16 hours. **A**. qRT-PCR analysis of *IFNA* and *IFNB* mRNA expression. **B**. IFNα and IFNβ secretion measured by ELISA. **C**. qRT-PCR analysis of IFN-stimulated genes mRNA expression. * $p<0.05$, ** $p<0.005$ (one-way ANOVA with Dunnett post-hoc test to correct for multiple comparisons). Data represent the mean ± SEM of 5 independent experiments with 2 donors in each. N.D., not detected.

Figure 4. TLR7-stimulated monocytes do not acquire a Th1-polarizing phenotype. **A**. qRT-PCR analysis of Th1-type and Th17-type mRNA gene expression by *ex vivo* isolated monocytes stimulated with 5 μg/ml IMQ, 2.5 μg/ml ssRNA40 or vehicle for 16 hours. **B**. ELISA analysis of cytokine secretion by monocytes stimulated with increasing concentrations of IMQ or ssRNA40 for 16 hours. **C**. Human $CD14^+$ monocytes were incubated ex vivo for 30 min with IRS661 (grey), IRS957 (white) or vehicle (black) and subsequently stimulated with IMQ, ssRNA40 or vehicle as in **A**. Cytokine secretion measured by ELISA after 16 hours. **D**. qRT-PCR analysis of Th17-type related genes (upper row) and Th1-type related genes (lower row) by monocytes stimulated with the TLR7-specific ligands Gardiquimod (GDQ) and Loxoribine (Loxo), with the TLR8-specific ligands ssRNA-DR and PolyU or vehicle as in **A**. **E**. qRT-PCR analysis of chemokines and cell surface receptor mRNA expression by monocytes stimulated as in **A**. **F**. Representative example of ICOSL and CD40 protein expression measured by flow cytometry on monocytes stimulated for

6 hours with IMQ (black line), ssRNA40 (black line) or vehicle (grey line) as compared to isotype control (grey curve). Numbers represent gMFI for vehicle (grey) versus TLR treatment (black). * p<0.05, ** p<0.005, ***p<0.001 (one-way ANOVA with Tukey's post-hoc test to correct for multiple comparisons for **A**, and **E)**. Data represent the mean ± SEM of 5 independent experiments with 2 donors in each. gMFI, geometric mean fluorescence intensity.

Figure 5. TLR7 and TLR8 differentially polarize CD4$^+$ T cells. **A** and **B**. Monocytes were stimulated with 5 μg/ml IMQ, 2.5 μg/ml ssRNA40 or vehicle for 16 hours and subsequently co-cultured with CD4$^+$ T cells at different monocyte:CD4 ratios for 72 hours. CD4$^+$ T cells were sorted by FACS and lysed. **A**. qRT-PCR analysis of Th1-, Th2-, Th17- and Treg cytokines and transcription factors mRNA at 24 hours. **B**. IFNγ and IL-17 secretion measured by ELISA at 72 hours. * p<0.05, ** p<0.005, ***p<0.001 (one-way ANOVA with Tukey's test for correction for multiple comparisons for **A**; two-way ANOVA with Tukey's post-hoc test to correct for multiple comparisons for **B**). Data are the mean ± SEM of 5 independent experiments with 2 donors in each.

Figure 6. TLR7 and TLR8 stimulation differentially activate MAPK and NFκB signaling. Monocytes were stimulated with IMQ, ssRNA40 or vehicle and expression of phosphorylated molecules was examined by FACS. **A**. Flow cytometric analysis of pMKK3/6, pMKK4/7, pMEK1/2 expression by monocytes stimulated with IMQ (grey thick like) or ssRNA40 (black fine line) as compared to isotype control (grey curve) after 15 min. **B**, **D**, **F**. Normalized (to gMFI at 0 min) expression of phosphorylated molecules at each time point. **C**. Flow cytometric analysis of pp38 and pERK1/2 expression by monocytes stimulated as in **A**, measured at 30 and 5 min, respectively. **E**. Flow cytometric analysis of pNFκB p65 and IκBα expression by monocytes stimulated as in **A** after 5, 30 and 45 min. For B, D and F data represents mean ± SEM analyzed

by two-way ANOVA with correction for multiple comparisons with Tukey's post-hoc test, showing statistical significance for IMQ- (star, *) or ssRNA40-stimulated (pound, #) monocytes as compared to 0 min. * $p<0.05$, ** $p<0.005$, ***$p<0.001$. N = 5 independent experiments with a total of 7 donors for **A**-**D** and 3 independent experiments with a total of 5 donors for **E** and **F**. gMFI, geometric mean fluorescence intensity.

Figure 7. TLR7-dependent FOSL1 expression inhibits Th1-type cytokines. **A**. qRT-PCR analysis of *ATF1*, *ATF2*, *FOSL1* and *FOSL2* mRNA expression by monocytes stimulated with IMQ (black), ssRNA40 (white) or vehicle. Data are normalized to vehicle-treated monocytes. qRT-PCR analysis of Th1-type cytokine mRNA gene expression (**B**) and ELISA measurement of protein secretion (**C**) by *ATF1*-, *ATF2*-, *FOSL1*- and *FOSL2*-silenced monocytes stimulated with IMQ (black) or vehicle (white) as compared to non-target-silenced control (NT). **D**. qRT-PCR analysis of *FOSL1* mRNA expression by monocytes stimulated with RNA viruses for 16 hours as compared to vehicle-treated monocytes. **E**. qRT-PCR analysis of *TNF* and *IL27* mRNA gene expression by *FOSL1*-silenced monocytes infected with IAV, MV, VSV, or left uninfected. * $p<0.05$, ** $p<0.005$, ***$p<0.001$ (one-way ANOVA with Tukey's post-hoc test to correct for multiple comparisons for **D**; two-way ANOVA with Tukey's post-hoc test for correction for multiple comparisons for **A**, **B**, **C**, and **E**). In **A**, statistical significance shown as star (*) for IMQ- and pound sign ($^{\#}$) for ssRNA40-stimulated monocytes as compared to vehicle treatment. In **B**, **C** and **E** significance is shown for target siRNA compared to NT siRNA and similar treatment. Data the mean $\pm$ SEM of 2 independent experiments with 2 donors in each for **A**, 4 independent experiments with a total of 6 donors for **B** and **C**, and 4 independent experiments with a total of 5 donors for **D** and **E**.

Figure 8. TLR7 does not induce a type I IFN response in human CD14^{+} monocytes. (**A** and **B**). Human CD14^{+} monocytes were stimulated ex vivo with IMQ (black circle), ssRNA40 (white

circle) or vehicle (white square) for 36 hours. **A**. qRT-PCR analysis of *IFNA* and *IFNB* mRNA gene expression. **B**. cytokine release measured by ELISA. (C and D). C. qRT-PCR analysis of IFNA and IFNB mRNA expression by monocytes stimulated with different concentrations of IMQ or ssRNA40 for 16 hours. **D**. Cytokine release examined by ELISA as compared to vehicle (dotted line). **E**. qRT-PCR analysis of ISGs mRNA expression by monocytes stimulated as in **A**. **F**. qRT-PCR analysis of *IFNA* and *IFNB* gene expression by monocytes stimulated with the TLR7-specific ligands (black bars) Gardiquimod (GDQ) and Loxoribine (Loxo), with the TLR8-specific ligands (grey bars) ssRNA-DR and PolyU or vehicle (white bar) for 16 hours. **G**. qRT-PCR analysis of *IFNA* and *IFNB* gene expression at 16 hours by monocytes incubated for 30 min with IRS661 (grey), IRS957 (white) or vehicle (black) and subsequently stimulated with IMQ, ssRNA40 or vehicle as in **A**. **H**. Representative flow cytometric analysis of pTBK1 and pIRF3 expression by monocytes stimulated with vehicle (grey curve), IMQ (thick grey line) or ssRNA40 (black thin line) for 15 and 30 min, respectively. Numbers represent gMFI for IMQ (grey) versus ssRNA40 treatment (black). **I**. Normalized (to gMFI at 0 min, dashed line) expression of phosphorylated molecules at different time points. * $p<0.05$, ** $p<0.005$, ***$p<0.001$ (two-way ANOVA with Tukey's test for correction for multiple comparisons for **A**, **B**, **E**, **G**, and **I**). In **A**, **B** and **E**, statistical significance is shown as stars (*) for ssRNA40-stimulated monocytes as compared to vehicle treatment at each time point. In **G**, statistical significance is shown for ssRNA40- or IMQ-treated monocytes as compared to vehicle-treated cells under the same stimulatory conditions (vehicle, IRS661 or IRS957). In **I**, statistical significance is shown for IMQ- (*) or ssRNA40-stimulated ($^{\#}$) monocytes as compared to 0 min. Data represent the mean $\pm$ SEM of 2 independent experiments with 2 donors in each for **A**-**G**, and 3 independent experiments with a total of 5 donors for **H**,**I**. gMFI, geometric mean fluorescence intensity.

Figure 8. TLR7-dependent Ca^{2+} signaling inhibits type I IFN response. **A**. Flow cytometric analysis of Ca^{2+} flux over time by monocytes stimulated (downward arrows) with various

concentrations of IMQ, ssRNA40 or ionomycin, assessed as the ratio of Indo-1AM fluorescence at 400 nm to that at 475 nm (400/475). **B**. Flow cytometry analysis of Ca^{2+} flux in monocytes pre-incubated for 30 min with control sequence (IRS Control, grey) or with the TLR7-specific inhibitory sequence IRS 661 (black) and subsequently stimulated with 5 μg/ml IMQ. **C.** Flow cytometric analysis of Ca^{2+} flux in monocytes pre-incubated for 30 min with EGTA (left panel, grey) or xestopongin C (right panel, grey) or vehicle (black), and subsequently stimulated with 5 μg/ml IMQ. (**D** to **G).** Monocytes were pre-incubated for 30 min with Quin-2 AM or vehicle and stimulated with IMQ or not for 16 hours. qRT-PCR analysis of *IFNA* and *IFNB* (D) and ISGs (E) mRNA gene expression. **F**. IFNα secretion measured by ELISA. **G**. qRT-PCR analysis of *IRF3* and *IRF7* mRNA gene expression. * p<0.05, ** p<0.005, ***p<0.001 (one-way ANOVA with Tukey's post-hoc test to correct for multiple comparisons). In **D** to **F**, stars denote statistical significance as compared to IMQ treatment. Data are a representative example of N = 5 independent experiments with one donor in each for **A**, **B** and **C**, and the mean ± SEM of 4 independent experiments with 2 donors in each for **E** and **F**, and one donor in each for **G**.

Figure 10. FOSL1 expression requires Ca^{2+} and ERK signaling. qRT-PCR analysis of *FOSL1* mRNA gene expression at 18 hours by $CD14^{+}$ monocytes pre-incubated for 30 min at 37°C with the p38 inhibitor SB203580 (**A**), the JNK inhibitor SP600125 (**B**), the ERK1/2 inhibitor SCH772984 (**C**) or the Ca^{2+} chelation agent Quin-2 AM (**D**), and stimulated with vehicle (white bars) or 2.5 μg/ml IMQ (grey bars). **E**. qRT-PCR analysis of *IFNA1* and *IFNA2* mRNA expression by *FOSL1*- or non-target (NT)-silenced monocytes stimulated with vehicle, IMQ or ssRNA40. Mean ± SEM of 4 independent experiments with one donor in each for A to D, and 3 independent experiments with a total of 5 donors for **E** . * p<0.05, ** p<0.001 (two-way ANOVA with Tukey's test to correct for multiple comparisons for **A** to **C**, and one-way ANOVA with Tukey's post-hoc test for correction for multiple comparisons for **D**.

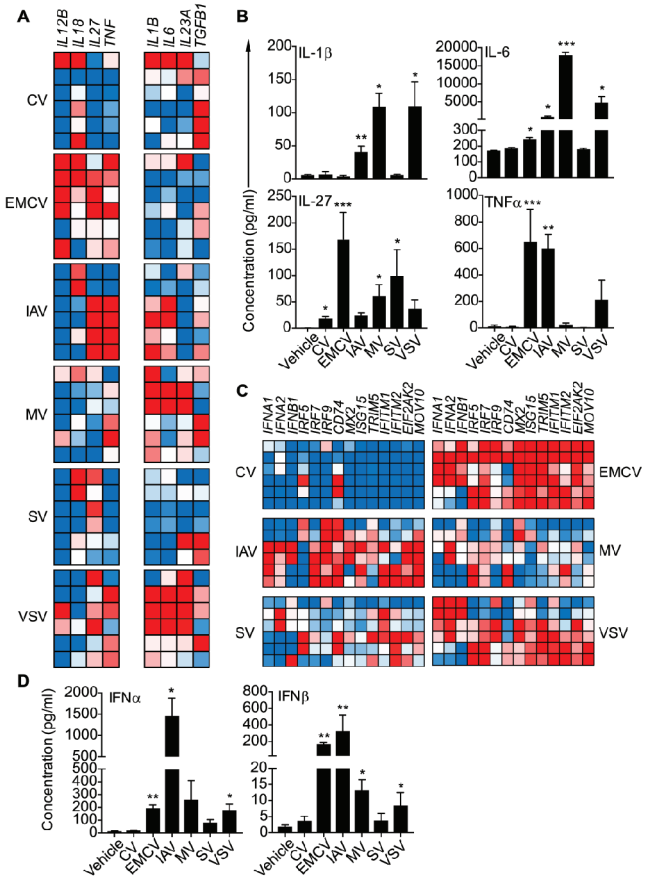
A
IL12B
IL18
IL27
TNF
IL1B
IL6
IL23A
TGFB1
CV
EMCV
IAV
MV
SV
VSV
B
IL-1β
IL-6
IL-27
TNFα
Concentration (pg/ml)
Vehicle
CV
EMCV
IAV
MV
SV
VSV
C
IFNA1
IFNA2
IFNB1
IRF5
IRF7
IRF9
CD74
MX2
ISG15
TRIM5
IFITM1
IFITM2
EIF2AK2
MCV10
D
IFNα
IFNβ
Concentration (pg/ml)

Figure 1

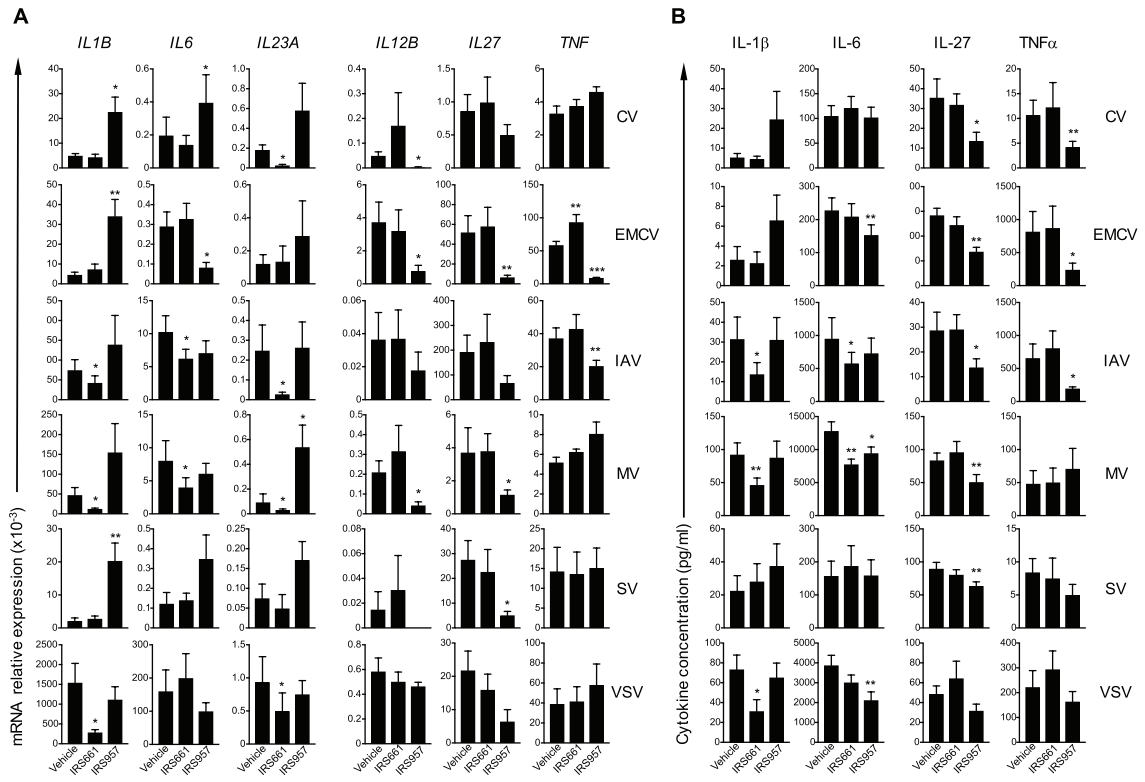
A
IL1B
IL6
IL23A
IL12B
IL27
TNF
CV
EMCV
IAV
MV
SV
VSV
mRNA relative expression (x10-3)
Vehicle
IRS661
IRS957
B
IL-1β
IL-6
IL-27
TNFα
Cytokine concentration (pg/ml)

Figure 2

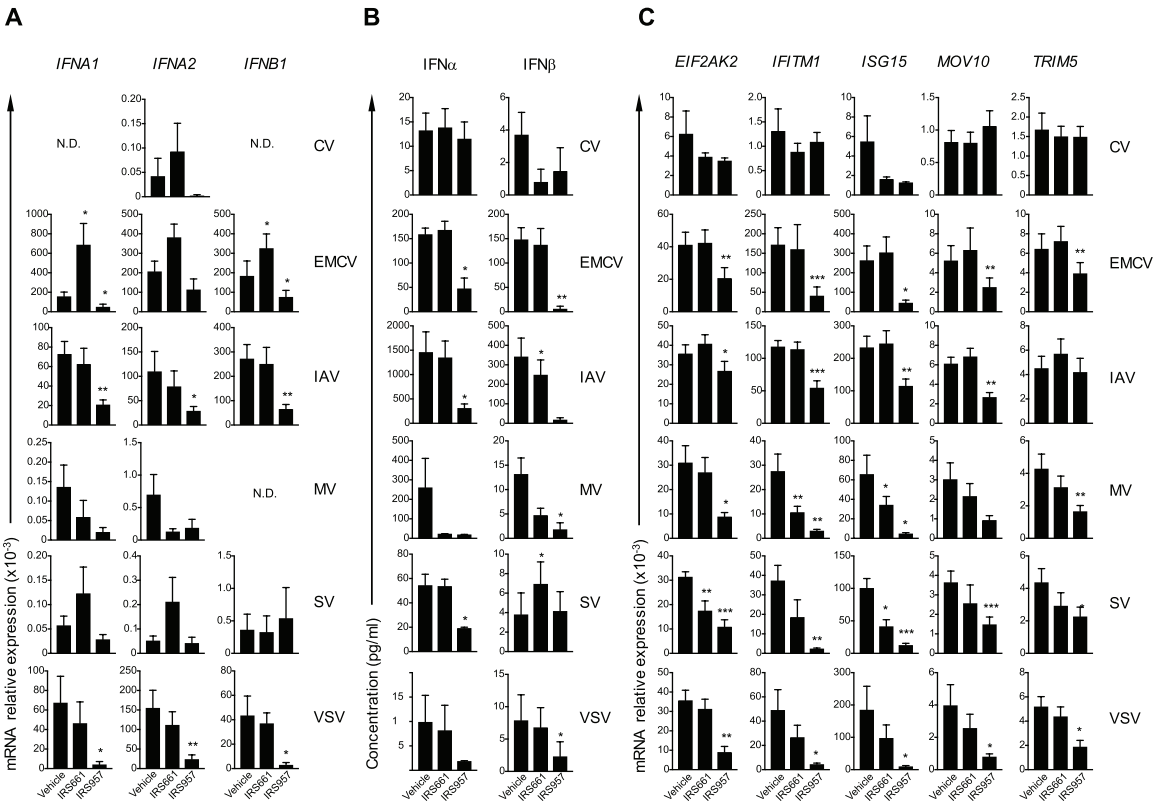
A
B
C
IFNA1
IFNA2
IFNB1
IFNα
IFNβ
EIF2AK2
IFITM1
ISG15
MOV10
TRIM5
CV
EMCV
IAV
MV
SV
VSV
N.D.
mRNA relative expression (x10-3)
Concentration (pg/ml)
Vehicle
IRS661
IRS957

Figure 3

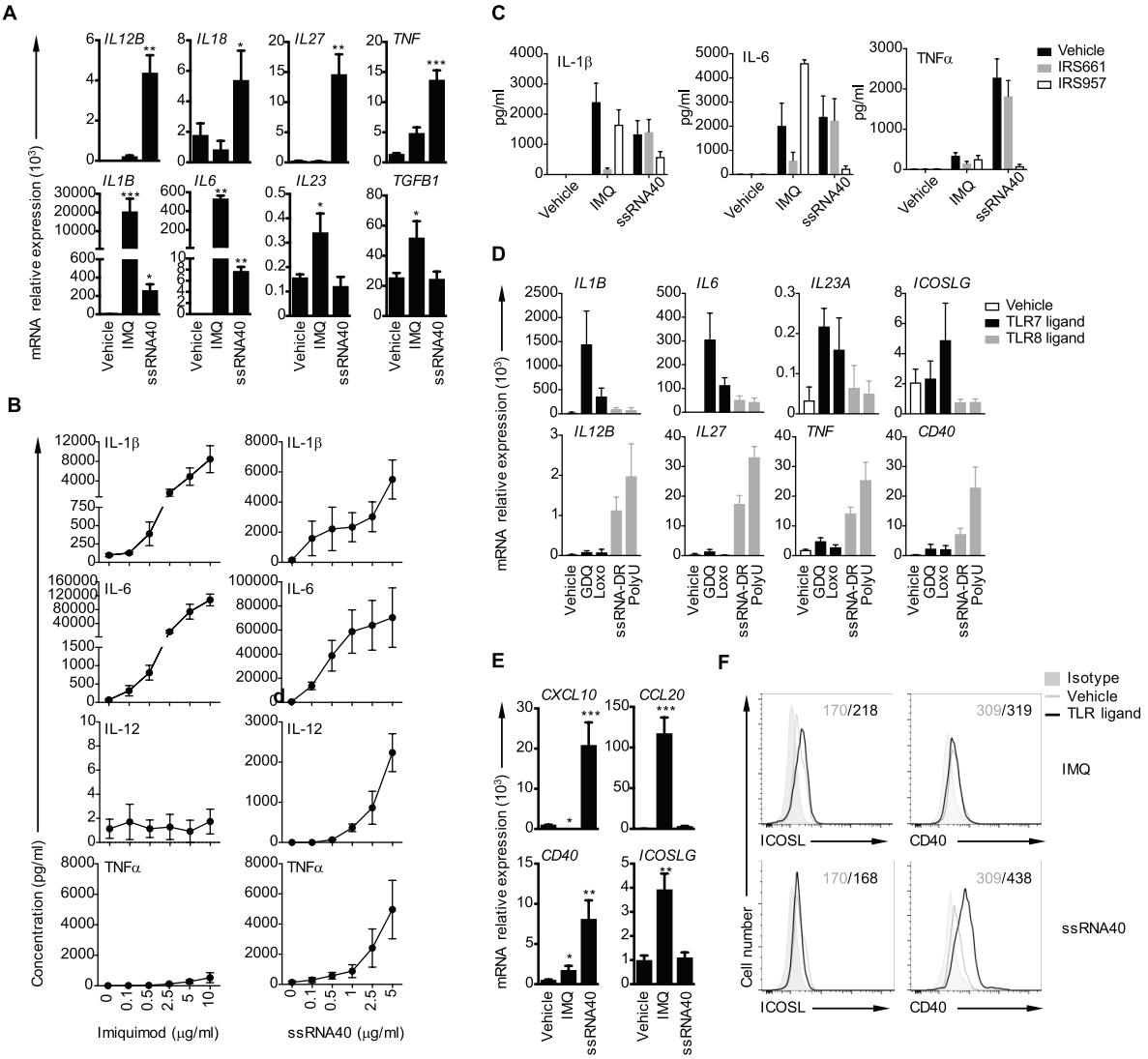
A
IL12B
IL18
IL27
TNF
IL1B
IL6
IL23
TGFB1
mRNA relative expression (10³)
Vehicle
IMQ
ssRNA40
B
IL-1β
IL-6
IL-12
TNFα
Concentration (pg/ml)
Imiquimod (μg/ml)
ssRNA40 (μg/ml)
C
IL-1β
IL-6
TNFα
pg/ml
Vehicle
IRS661
IRS957
D
IL1B
IL6
IL23A
ICOSLG
IL12B
IL27
TNF
CD40
mRNA relative expression (10³)
Vehicle
TLR7 ligand
TLR8 ligand
Vehicle
GDQ
Loxo
ssRNA-DR
PolyU
E
CXCL10
CCL20
CD40
ICOSLG
mRNA relative expression (10³)
Vehicle
IMQ
ssRNA40
F
Isotype
Vehicle
TLR ligand
170/218
309/319
IMQ
170/168
309/438
ssRNA40
ICOSL
CD40
Cell number

Figure 4

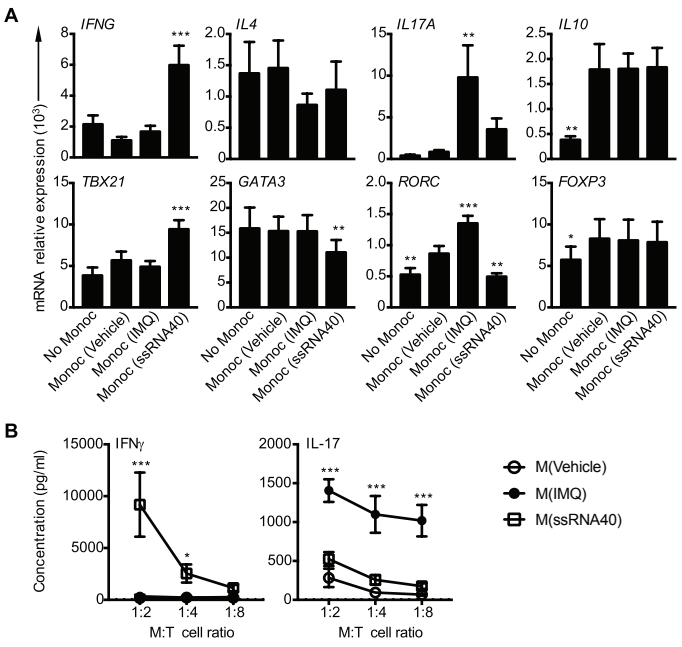
A
IFNG
IL4
IL17A
IL10
TBX21
GATA3
RORC
FOXP3
mRNA relative expression (10³)
No Monoc
Monoc (Vehicle)
Monoc (IMQ)
Monoc (ssRNA40)
B
IFNγ
IL-17
Concentration (pg/ml)
M:T cell ratio
1:2
1:4
1:8
M(Vehicle)
M(IMQ)
M(ssRNA40)

Figure 5

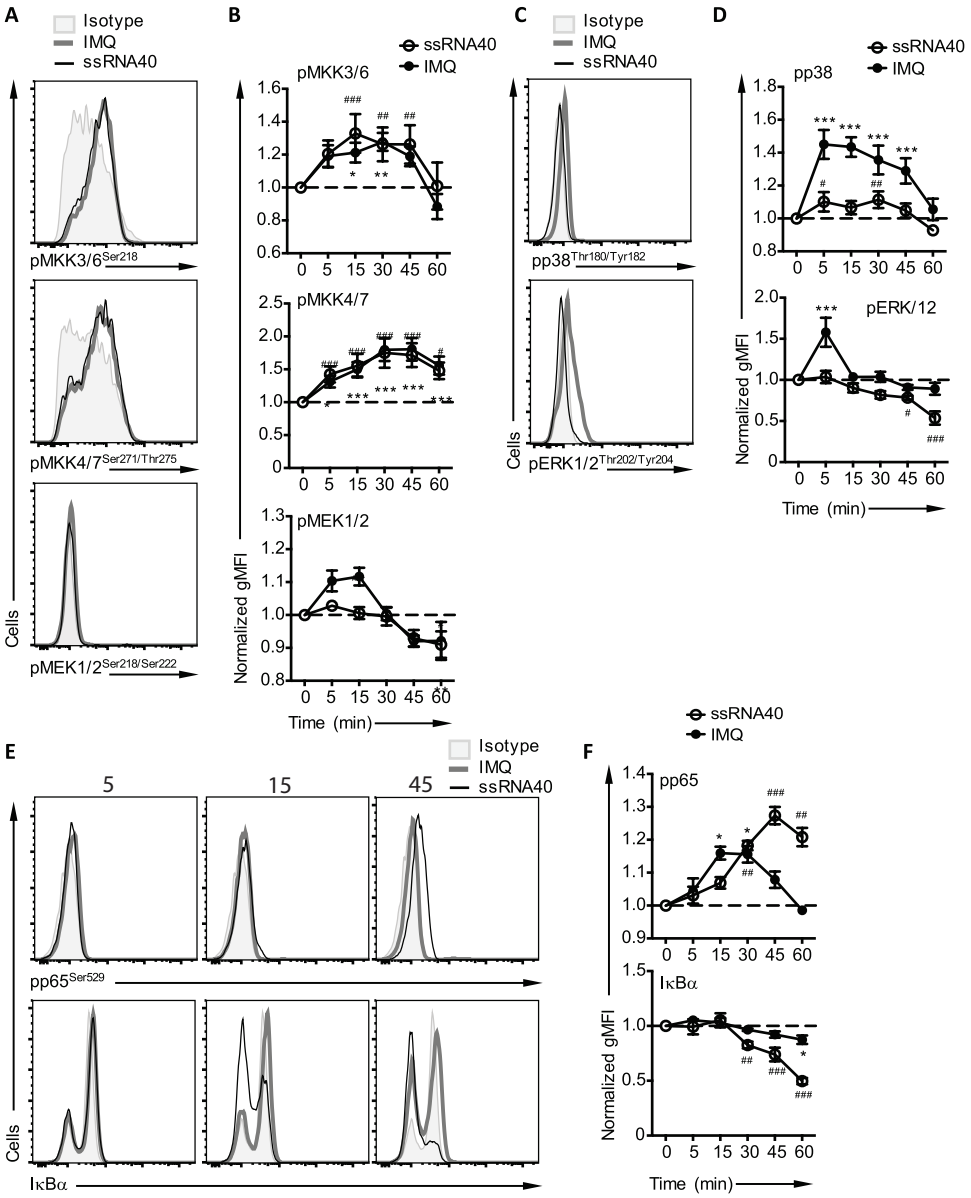
A
Isotype
IMQ
ssRNA40
pMKK3/6Ser218
pMKK4/7Ser271/Thr275
pMEK1/2Ser218/Ser222
Cells
B
ssRNA40
IMQ
pMKK3/6
pMKK4/7
pMEK1/2
Normalized gMFI
Time (min)
C
Isotype
IMQ
ssRNA40
pp38Thr180/Tyr182
pERK1/2Thr202/Tyr204
Cells
D
ssRNA40
IMQ
pp38
pERK/12
Normalized gMFI
Time (min)
E
Isotype
IMQ
ssRNA40
5
15
45
pp65Ser529
IκBα
Cells
F
ssRNA40
IMQ
pp65
IκBα
Normalized gMFI
Time (min)

Figure 6

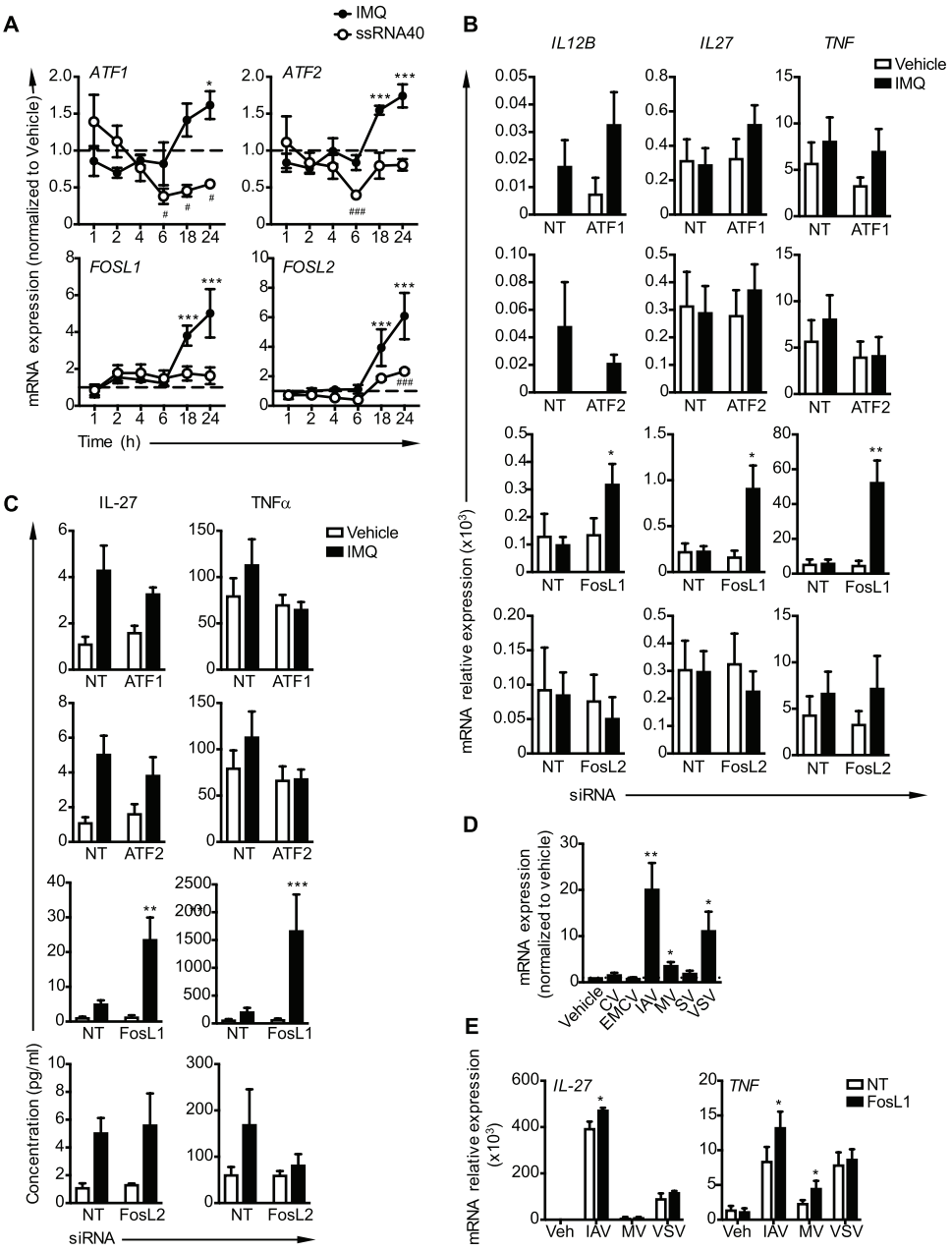
A
IMQ
ssRNA40
ATF1
ATF2
FOSL1
FOSL2
mRNA expression (normalized to Vehicle)
Time (h)
B
IL12B
IL27
TNF
Vehicle
IMQ
NT
ATF1
ATF2
FosL1
FosL2
mRNA relative expression (x10³)
siRNA
C
IL-27
TNFα
Vehicle
IMQ
Concentration (pg/ml)
siRNA
D
mRNA expression (normalized to vehicle)
Vehicle
CV
EMCV
IAV
MV
SV
VSV
E
IL-27
TNF
NT
FosL1
mRNA relative expression (x10³)
Veh
IAV
MV
VSV

Figure 7

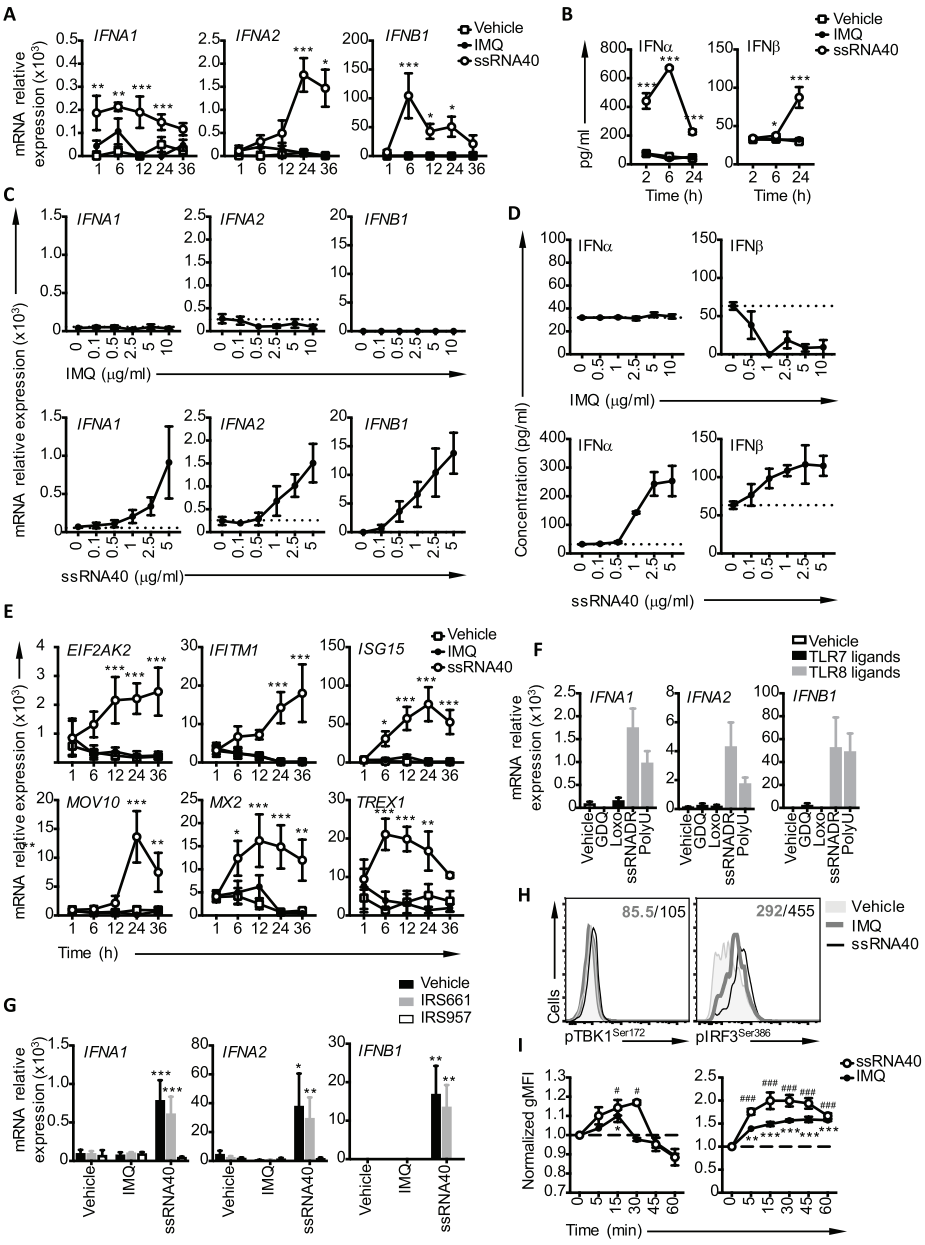
A
IFNA1
IFNA2
IFNB1
Vehicle
IMQ
ssRNA40
mRNA relative expression (x10³)
B
IFNα
IFNβ
pg/ml
Time (h)
C
IMQ (μg/ml)
ssRNA40 (μg/ml)
D
Concentration (pg/ml)
E
EIF2AK2
IFITM1
ISG15
MOV10
MX2
TREX1
Time (h)
F
TLR7 ligands
TLR8 ligands
Vehicle
GDQ
Loxo
ssRNADR
PolyU
G
IRS661
IRS957
H
85.5/105
292/455
Cells
pTBK1Ser172
pIRF3Ser386
I
Normalized gMFI
Time (min)

Figure 8

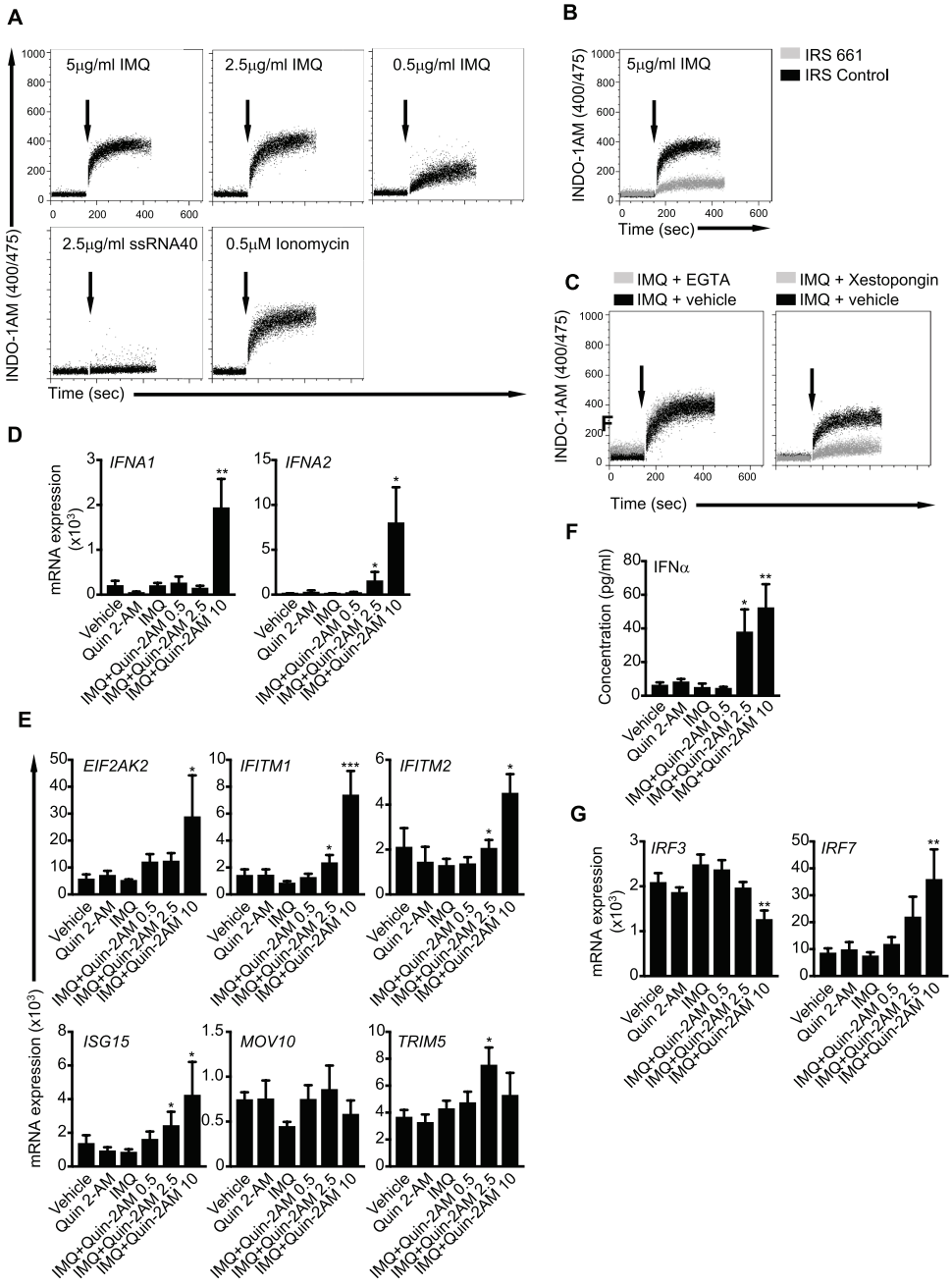
A
5μg/ml IMQ
2.5μg/ml IMQ
0.5μg/ml IMQ
2.5μg/ml ssRNA40
0.5μM Ionomycin
INDO-1AM (400/475)
Time (sec)
B
5μg/ml IMQ
IRS 661
IRS Control
INDO-1AM (400/475)
Time (sec)
C
IMQ + EGTA
IMQ + vehicle
IMQ + Xestopongin
IMQ + vehicle
INDO-1AM (400/475)
Time (sec)
D
IFNA1
IFNA2
mRNA expression (x10³)
Vehicle
Quin 2-AM
IMQ
IMQ+Quin-2AM 0.5
IMQ+Quin-2AM 2.5
IMQ+Quin-2AM 10
E
EIF2AK2
IFITM1
IFITM2
ISG15
MOV10
TRIM5
mRNA expression (x10³)
F
IFNα
Concentration (pg/ml)
G
IRF3
IRF7
mRNA expression (x10³)

Figure 9

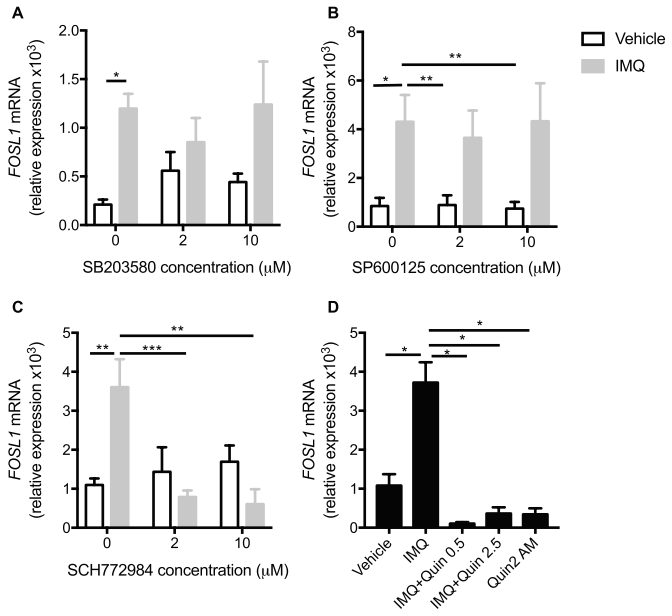
A
B
C
D
FOSL1 mRNA (relative expression x10^3)
SB203580 concentration (μM)
SP600125 concentration (μM)
SCH772984 concentration (μM)
Vehicle
IMQ
Vehicle
IMQ
IMQ+Quin 0.5
IMQ+Quin 2.5
Quin2 AM

Figure 10

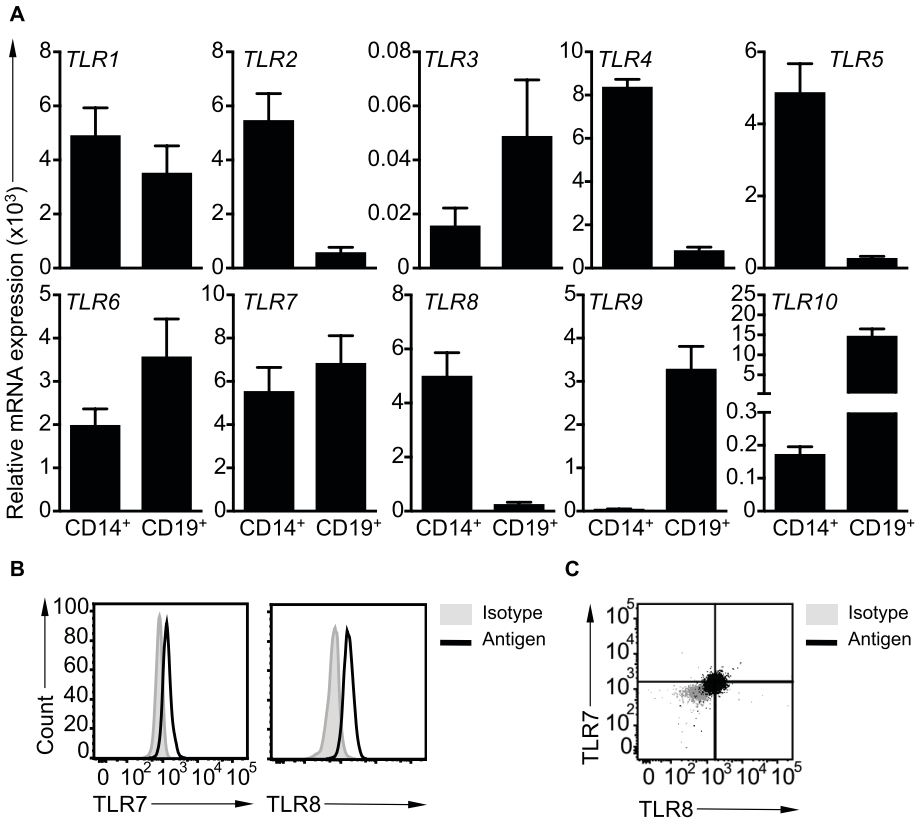

Supplementary Figure 1. Expression of TLR7 and TLR8 by human CD14$^+$ monocytes. **A**. qRT-PCR analysis of *TLR1-10* gene expression by *ex vivo* isolated CD14$^+$ monocytes and CD19$^+$ B cells. **B** and **C**. Example of flow cytometric analysis of TLR7 and TLR8 (black) protein expression as compared to isotype control (grey). Data represent mean ± SEM of 3 independent experiments with 2 donors in each for **A**, and a representative example of 3 independent experiments with 1 donor in each for **B** and **C**.

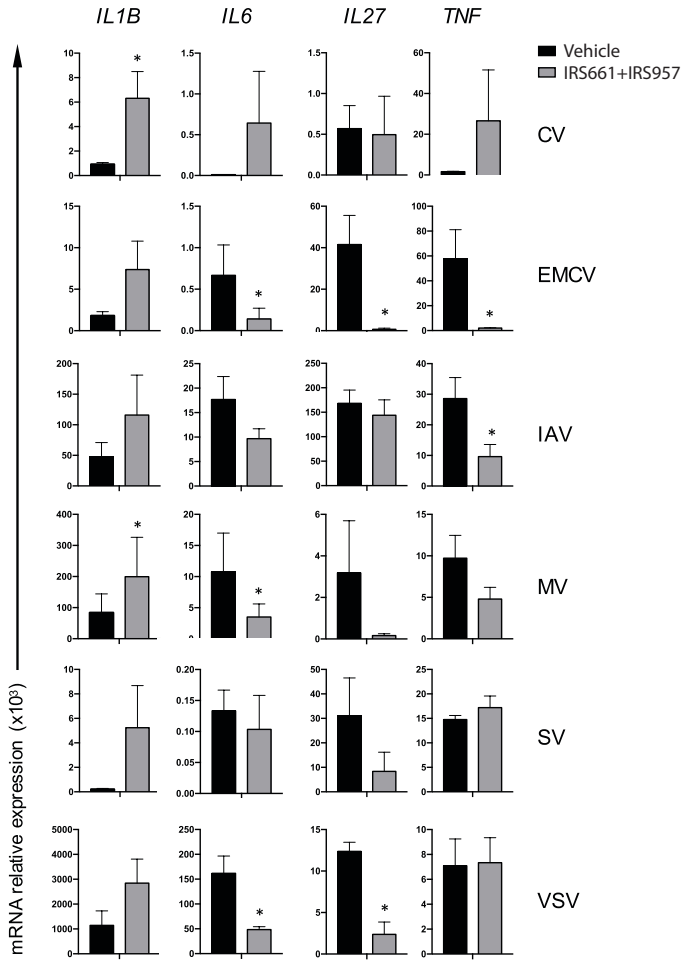

Supplementary Figure 2. TLR7 and TLR8 blockade and virus infection. qRT-PCR analysis of *IL1B*, *IL6*, *IL27* and *TNF* mRNA gene expression by $CD14^+$ monocytes pre-incubated for 30 min with IRS661 and IRS957 and subsequently stimulated with Coxsackievirus (CV), Encephalomyocarditis virus (EMCV), Influenza A virus (IAV), Measles virus (MV), Sendai virus (SV) and Vesicular Stomatitis virus (VSV) for 16 hours. * $p<0.05$ (t-test). Mean ± SEM of 4 independent experiments with 1 donor in each.

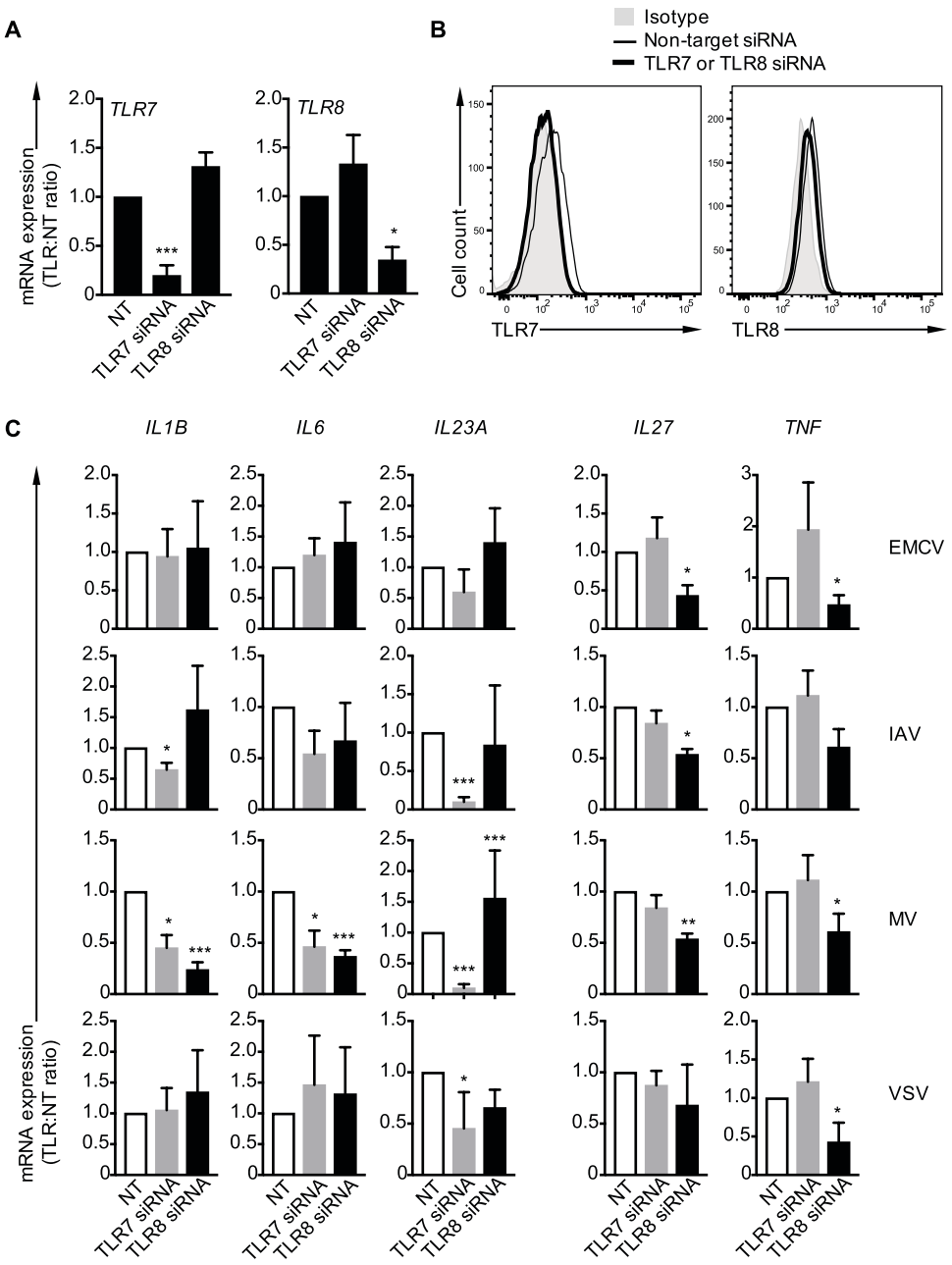

Supplementary Figure 3. Cytokine expression by TLR7- and TLR8-silenced monocytes after RNA virus infection. (**A** to **C**). Ex vivo isolated monocytes were transfected with siRNAs targeting TLR7, TLR8, or a non-specific target (NT). **A**. qRT-PCR analysis of *TLR7* and *TLR8* gene expression in NT-, TLR7- and TLR8-silenced monocytes normalized to NT. **B**. Flow cytometric analysis example of TLR7 and TLR8 protein expression by TLR-silenced (thick black line) and control (thin black line) monocytes as compared to isotype (grey curve). **C**. qRT-PCR analysis of cytokine mRNA gene expression by TLR7- (grey), TLR8- (black) and NT-silenced (white) monocytes infected with EMCV, IAV, MV and VSV at MOI = 5 for 16 hours; data shown are normalized to NT. * $p<0.05$, ** $p<0.005$, ***$p<0.001$ (one-way ANOVA with Dunnett test for correction for multiple comparisons). Data correspond to mean ± SEM of 8 independent experiments with a total of 10 donors for **A**, 3 independent experiments with one donor in each for **B**, and mean ± SEM of 4 independent experiments with a total of 5 donors for **C**.

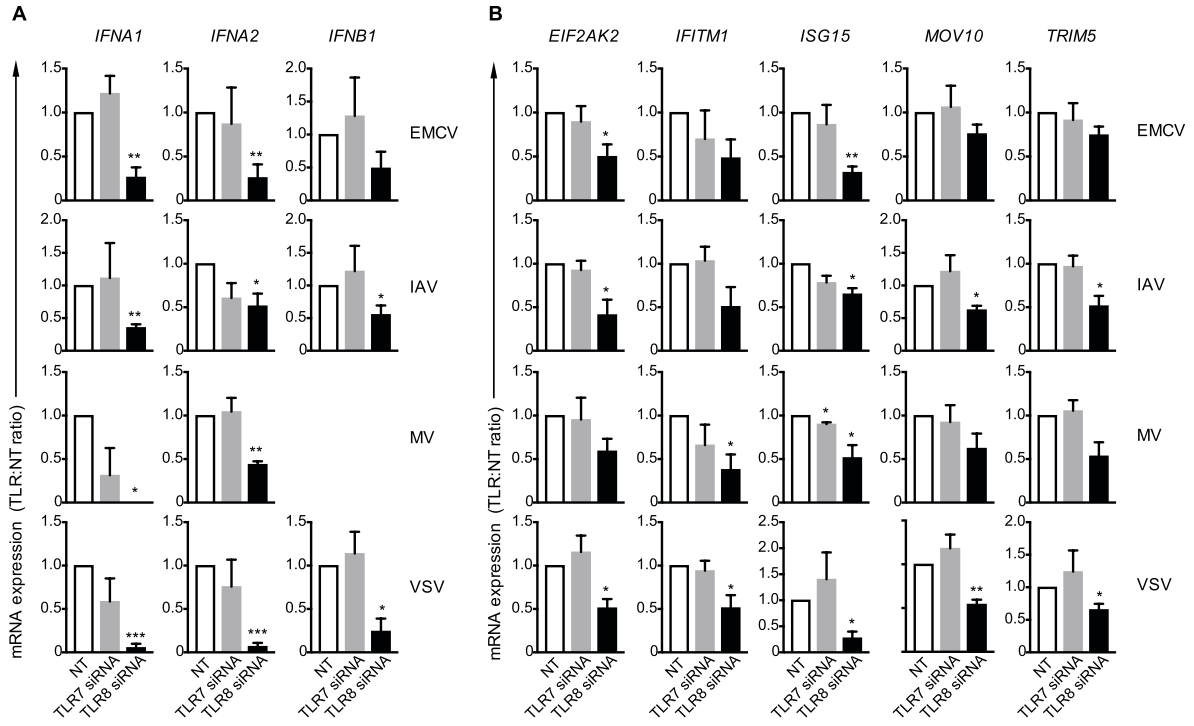

Supplementary Figure 4. Type I IFN response by TLR7- and TLR8- silenced monocytes after RNA virus infection. *Ex vivo* isolated monocytes were transfected with siRNAs targeting TLR7, TLR8, or a non-specific target (NT) and 36 hours later they were infected with EMCV, IAV, MV and VSV at MOI = 5 for 16 hours. Normalized (to NT) *IFNA* and *IFNB* (**A**) and ISGs (**B**) expression in NT- (white), TLR7- (grey) and TLR8-silenced (black) monocytes. * $p<0.05$, ** $p<0.005$, ***$p<0.001$ (one-way ANOVA with Dunnett test for correction for multiple comparisons). Mean ± SEM of N = 4 independent experiments with one donor in each.

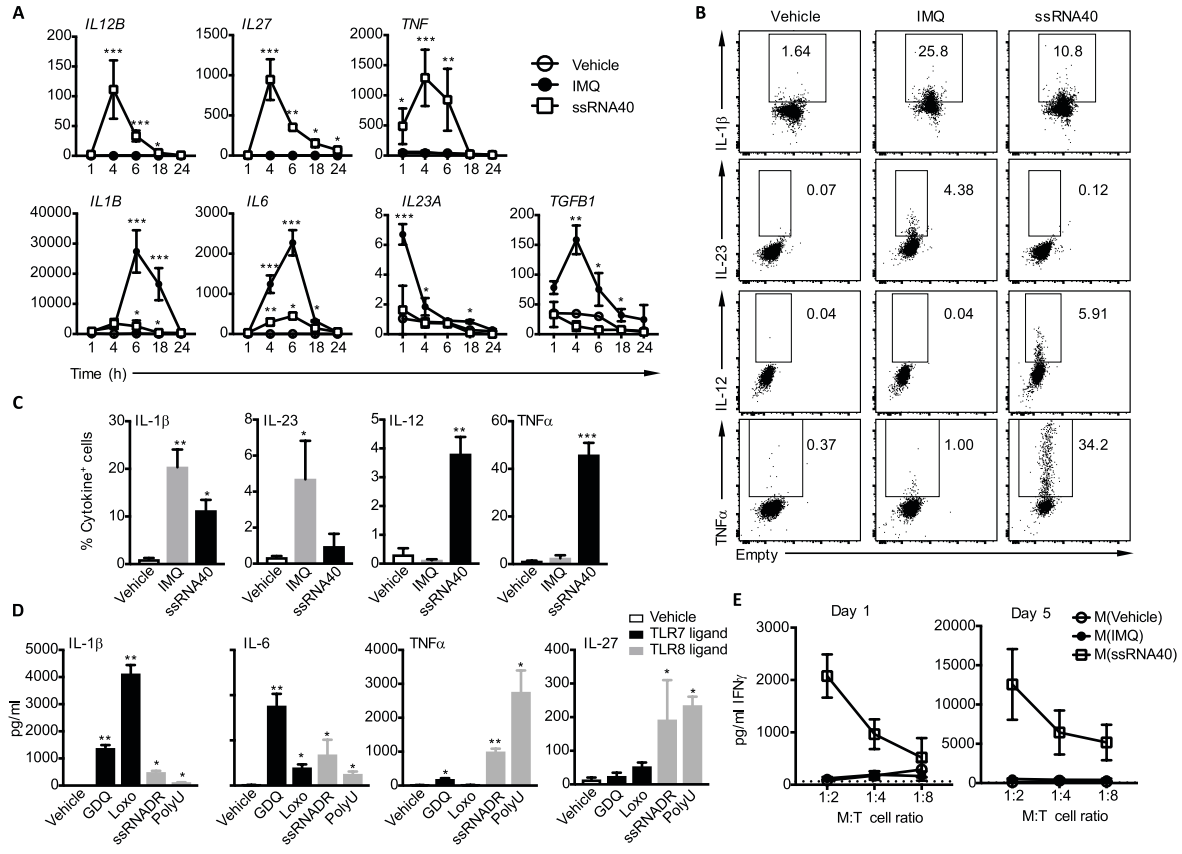

Supplementary Figure 5. Th1- and Th17-polarizing phenotype after TLR7 and TLR8 activation in human monocytes. **A**. qRT-PCR analysis of Th1- and Th17-type cytokine gene expression by human $CD14^+$ monocytes stimulated with IMQ (black circle), ssRNA40 (white square) or vehicle (white circle) for 24 hours. **B**. Flow cytometric analysis of IL-1β, IL-23, IL-12 and TNFα protein expression by monocytes stimulated with vehicle, IMQ or ssRNA40 for 8 hours in the presence of GolgiStop. Numbers in dot plots represent frequency of cytokine-producing monocytes from total $CD14^+$ cells. **C**. Frequency of cytokine-producing monocytes (as in **B**). **d**. Secretion of Th17-and Th1-type related cytokines measured by ELISA by monocytes stimulated with the TLR7-specific ligands Gardiquimod (GDQ) and Loxoribine (Loxo), with the TLR8-specific ligands ssRNA-DR and PolyU or vehicle for 16 hours. **E**. IFNγ secretion measured by ELISA from monocytes previously stimulated with IMQ (black circle), ssRNA40 (white square) or vehicle (white circle) for 16 hours and co-cultured with $CD4^+$ T cells at different monocyte:CD4 ratios for 1 and 5 days. * $p<0.05$, ** $p<0.005$, ***$p<0.001$ (one-way ANOVA with Tukey's post-hoc test to correct for multiple comparisons for **C** and **D**; two-way ANOVA with correction for multiple comparisons with Tukey's test for **A** and **E**). In **A**, statistical significance is shown as compared to vehicle at each time point. In **E**, statistical significance is shown as compared to vehicle-treated monocyte:$CD4^+$ T cell co-culture at each monocyte:$CD4^+$ T cell ratio. Mean ± SEM of N = 5 experiments with a total of 7 donors in **A**, one representative example of 3 independent experiments with one donor in **B**, mean ± SEM of 3 independent experiments with one donor in **C**, 4 independent experiments with a total of 6 donors in **D**, and 5 independent experiments with 2 donors in each in **E**.

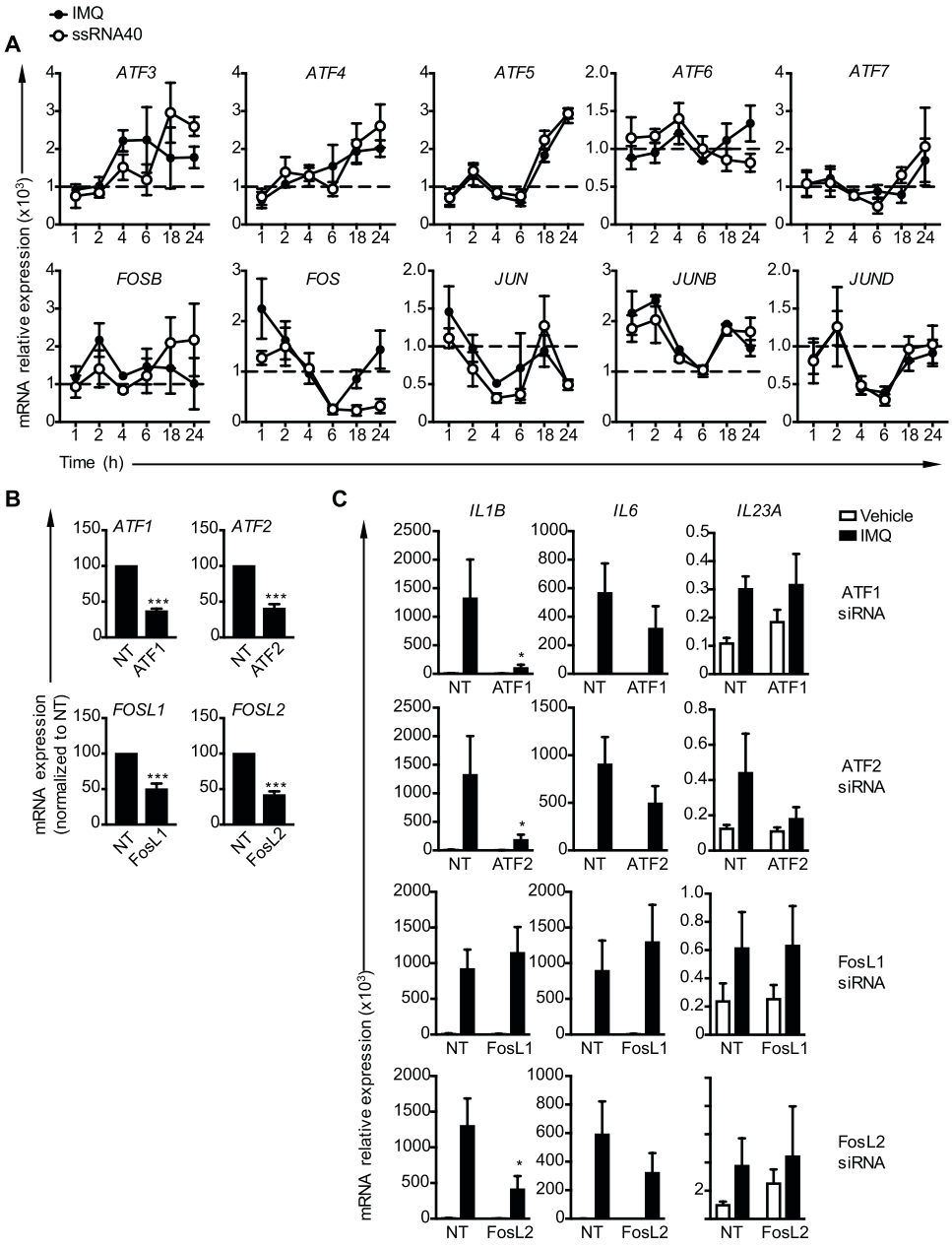

Supplementary Figure 6. Redundant roles of ATF1, ATF2 and FOSL2 in inducing Th17-type cytokines after TLR7 stimulation. **A**. qRT-PCR analysis of AP-1 subunits mRNA expression by monocytes stimulated with IMQ (black), ssRNA40 (white) or vehicle (dashed line) for 24 hours. Data shown are normalized to vehicle-treated monocytes at each time point. **B**. qRT-PCR analysis of *ATF1*, *ATF2*, *FOSL1* and *FOSL2* mRNA expression by monocytes transfected with siRNAs targeting *ATF1*, *ATF2*, *FOSL1*, *FOSL2* or a non-specific target (NT). Data shown are normalized (to NT). **C**. qRT-PCR analysis of *IL1B*, *IL6* and *IL23* mRNA gene expression by *ATF1*-, *ATF2*-, *FOSL1*-, *FOSL2*- and NT-silenced monocytes stimulated for 12 hours with IMQ (black) or vehicle (white). *p<0.05, ***p<0.001 (two-way ANOVA with Tukey's post-hoc test for correction for multiple comparisons for **A** and **C**; paired t-test for **B**). In **A**, statistical significance is shown as compared to vehicle at each time point. For **C**, statistical significance is shown for target siRNA compared to NT siRNA and similar treatment (either IMQ or vehicle stimulation). Data shown as mean ± SEM of N = 2 independent experiments with 2 donors in each for **A** and 4 independent experiments with a total of 6 donors for **B** and **C**.

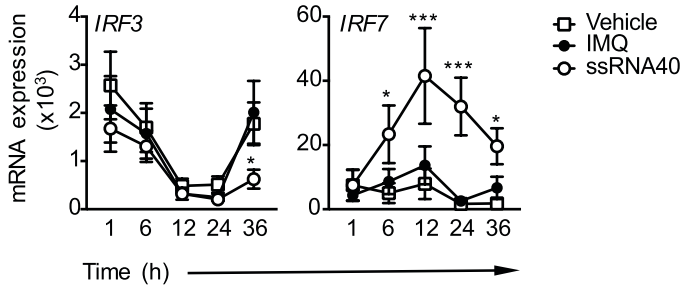

Supplementary Figure 7. Kinetics of IRF3 and IRF7 expression after TLR7 and TLR8 stimulation. qRT-PCR analysis of *IRF3* and *IRF7* gene expression by monocytes stimulated with IMQ (black), ssRNA40 (white) or vehicle (white square) for 36 hours. *p<0.05, ***p<0.001 (two-way ANOVA with Tukey's test to correct for multiple comparisons). Statistical significance is shown as compared to vehicle at each time point. Data are mean ± SEM of N = 3 independent experiments with a total of 5 donors.

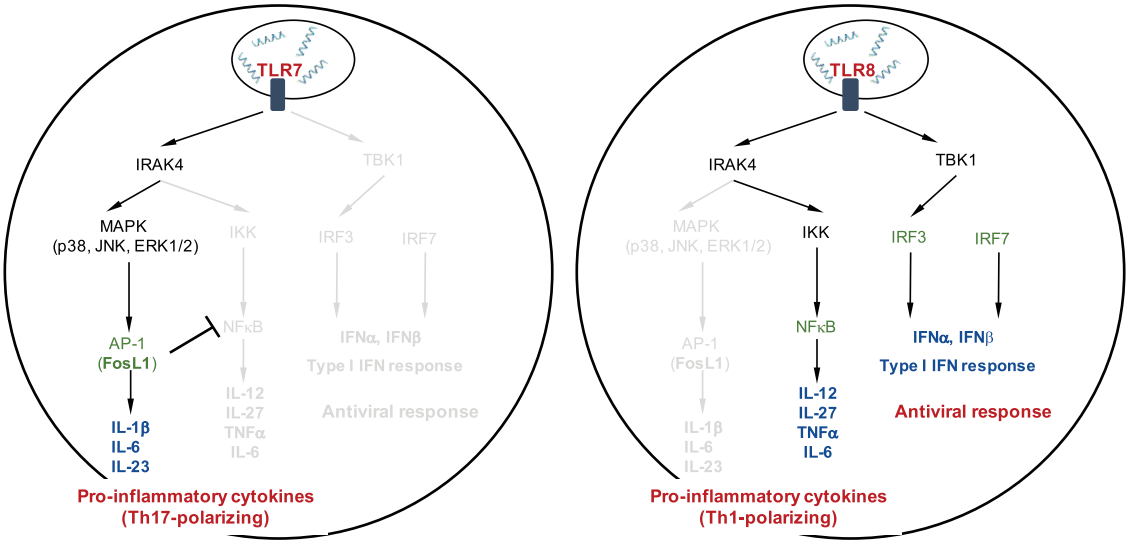

Supplementary Figure 8. Schematic of TLR7 and TLR8 signaling in human CD14$^+$ monocytes. Summary of TLR7 and TLR8 signaling differences in human CD14$^+$ monocytes identified in this work.